

QATAR UNIVERSITY

COLLEGE OF ENGINEERING

DEVELOPMENT OF AN AIR-COOLED INDUCTION MANIFOLD FOR INTERNAL

COMBUSTION ENGINES

BY

MOHAMED H. ELRENTISY

A Thesis Submitted to
the College of Engineering
in Partial Fulfillment of the Requirements for the Degree of
Masters of Science in Mechanical Engineering

January 2020

© 2019 MOHAMED H. ELRENTISY. All Rights Reserved.

COMMITTEE PAGE

The members of the Committee approve the Thesis of
MOHAMED H. ELRENTISY defended on 09/12/2019.

Dr. Samer Ahmad
Thesis/Dissertation Supervisor

Dr. Saud Abdu Ghani
Committee Member

Dr. Mahmoud Khader
Committee Member

Mostafa Elsharqawy
Committee Member

Add Member

Approved:

Dr. Khalid Kamal Naji, Dean, College of Engineering

ABSTRACT

ELRENTISY, MOHAMED, H, Masters : January : 2020,

Masters of Science in Mechanical Engineering

Title: Development of an Air-Cooled Induction Manifold for Internal Combustion Engines

Supervisor of Thesis: Samer A. Fikry.

Extreme weather conditions in the Arabian Gulf such as Qatar tends to be humid and high in temperature mostly throughout the year and this affects the performance of the vehicles' engines negatively, especially diesel engines. Moreover, it increases engines' exhaust emissions which in return maximizes greenhouse effect. Consequently, many studies have been conducted for innovating and testing new designs for controlling the ambient conditions at the inlet manifold of diesel engines; consequently enhancing engine's performance characteristics. In this project, different systems were designed for controlling inlet air temperature. The design of systems were captured from earlier studies investigating the effect of inlet ambient conditions on automobiles.

The experimental tool used for this project is a naturally aspirated single cylinder diesel engine test bed modified with a controlled air-cooled induction manifold. The test investigates the effect of running the engine at different controlled inlet air temperatures and observes engine's performance and emission characteristics. Furthermore, this study aims to track in-cylinder pressure relative to crank angle via a GW-Instek digital storage oscilloscope in addition to analyze the gained power after utilizing the cooling system.

It was found that running the diesel engine at lower inlet air temperature can maximize in-cylinder maximum pressure by 60% and increase the volumetric efficiency by 11%. It was also concluded that using the cooling system justifies its consumed power as the net gained power has increased by 12% due to increase of the drawn air density which resulted in a better fuel-injection atomization and more complete combustion.

DEDICATION

This work is dedicated to my wife who has always supported me through my educational life and pushed me beyond my limits as well as my parents who will always be my inspiration towards success.

ACKNOWLEDGMENTS

I am so grateful for the support I had in completing this project especially from Engineer Ihab Nabil who has been my best colleague during the entire project life cycle. I also would like to show my appreciation to my supervisor, Dr. Samer Fikry who has guided me during the project and provided me all the resources needed to complete the research.

My thanks to my colleagues; Mr. Ahmad Abdulla, Ahmad Sager, Yahia and Abubaker who have supported me through the experimental setup and data acquisition. Above all, I give praise to Allah for his never-ending blessings.

TABLE OF CONTENTS

DEDICATION	v
ACKNOWLEDGMENTS	vi
LIST OF TABLES	x
LIST OF FIGURES	xii
CHAPTER 1: INTRODUCTION	1
1.1 Background	1
1.1.1 Effect of ambient conditions on diesel engines.....	1
1.1.2 Approaches for controlling inlet air temperatures into ICE.....	2
1.2 Motivation behind the project	2
1.3 Research Objectives	3
1.4 Research methodology	3
1.5 Thesis structure	6
CHAPTER 2: LITERATURE REVIEW	7
2.1 Diesel engine	7
2.2 Engine performance characteristics	8
2.2.1 Engine power.....	8
2.2.2 Brake Specific Fuel Consumption (BSFC)	9
2.2.3 Break Mean Effective Pressure (BMEP).....	9
2.3 Effect of Ambient conditions on ICEs (QATAR CLIMATE).....	10

2.3.1 Humidity	10
2.3.2 Inlet Air Temperature	11
2.3.3 Volumetric Efficiency Improvements	13
2.4 Air conditioning system in cars.....	13
2.4.1 How does it work?.....	13
2.4.2 Intercooling concepts and effects	15
2.5 Experimental test rigs for ICEs	17
2.6 Inlet Manifolds	26
2.7 Outcomes of the Literature reviews	26
CHAPTER 3: EXPERIMENTAL SETUP	28
3.1 Experimental Method.....	28
3.2 Measuring Devices	37
3.2.1 The Oscilloscope	38
3.2.2 Pressure Transducer.....	39
3.2.3 Gas Analyzer	40
3.2.4 The Smoke Meter	42
3.2.5 Speed Tachometer	43
3.2.6 Anemometer	44
3.2.7 Temperature Humidity Meter.....	45
3.2.8 Clamp ampere meter.....	46

3.3 Safety Rules.....	47
CHAPTER 4: RESULTS AND DISCUSSIONS	48
4.1 Effect of varying inlet temperature on engine performance	48
4.1.1 Combustion Characteristics	48
4.1.2 Performance Characteristics.....	58
4.2 Effect of varying inlet temperature on emissions and smoke	72
4.2.1 Constant Load.....	72
4.2.2 Constant Speed	77
CHAPTER 5: CONCLUSION	81
REFERENCES	82
APPENDIX A: CALIBRATION CERTIFICATES	85
APPENDIX B: MATLAB CODINGS	87

LIST OF TABLES

Table 1. Section1 for data acquisition.....	4
Table 2. Section 2 for data acquisition.....	4
Table 3. Specifications of marine diesel engine [12].....	18
Table 4. External A/C system specifications [12]	18
Table 5. Effect of different inlet temperatures on diesel engine performance [13].....	20
Table 6. Turbocharged SI Test engine [14]	21
Table 7. Gasoline engine's specifications [15].....	23
Table 8. Spark assisted compression ignition engine specifications [16].....	25
Table 9. Specification of diesel engine test bed.....	29
Table 10. Technical specifications of the air conditioning compartment	33
Table 11. Technical specificaitons of the cooling system	34
Table 12. Gas Analyzer sensors and accuracy ranges	41
Table 13: Technical Specifications of the Smoke Meter	43
Table 14: Technical specifications of the speed tachometer	44
Table 15: Technical specification of the anemometer	45
Table 16: Specifications and performance of the temperature humidity meter.....	45
Table 17. Specifications and performance of the clamp ampere meter.....	46
Table 18. Uncertainty Table for calculated parameters	50
Table 19. Gained power for $T1 = 25^{\circ}\text{C}$ at constant load.	62
Table 20: Gained power for $T2 = 20^{\circ}\text{C}$ at constant load	62
Table 21. Gained energy for $T1 = 25^{\circ}\text{C}$ at constant load	64
Table 22: Gained energy for $T2 = 20^{\circ}\text{C}$ at constant load	64
Table 23: Gained power for $T1 = 25^{\circ}\text{C}$ at constant speed.....	69

Table 24: Gained power for $T_2 = 20^\circ\text{C}$ at constant speed.....	69
Table 25: Gained energy for $T_1 = 25^\circ\text{C}$ at constant speed.....	71
Table 26: Gained energy for $T_2 = 20^\circ\text{C}$ at constant speed.....	71

LIST OF FIGURES

Figure 1. Research methodology steps	5
Figure 2. Effect of inlet air temperature on fuel consumption [4]	9
Figure 3. Effect of humidity on engine efficiency and NOx level [6]	11
Figure 4. Annual average temperature distribution in Qatar [7]	12
Figure 5. Combustion efficiency against different ambient temperature and humidity [6]	12
Figure 6. Schematic shows the components of vapor compression cycle [10]	14
Figure 7. Schematic of Air-to-Air Intercooler [11]	16
Figure 8. Schematic of Water-to-Air Intercooler [11]	17
Figure 9. Schematic of experimental apparatus	19
Figure 10. Cylinder pressure variation of three different inlet temperatures [13]	20
Figure 11. Test Setup 1 consisting of two heat exchangers [14]	22
Figure 12. Test setup 2 with improved intercooler/evaporator system [14]	22
Figure 13. Detailed schematic diagram of the engine's setup [15]	24
Figure 14. Effect of inlet air temperature on rate of heat release [16]	25
Figure 15. Schematic of Test Rig	28
Figure 16: Dynamometer coupled to the crankshaft of the engine	30
Figure 17: Control Board including all Main Switches	30
Figure 18. Fuel Tanks	31
Figure 19. Fuel calibrated burette	32
Figure 20. Fuel supply valves	32
Figure 21. Air conditioning compartment	35
Figure 22. Design of an air cooled induction manifold	36

Figure 23. GW-Instek oscilloscope (Model GDS-3152)	38
Figure 24. Waveform displayed on oscilloscope's screen	38
Figure 25. Pressure transducer and charge converter	39
Figure 26: Pressure transducer	39
Figure 27. Pressure transducer calibration.....	40
Figure 28: ENERAC model 700 integrated emissions	40
Figure 29. Smoke meter overview	42
Figure 30. Smoke meter ports	42
Figure 31. Speed tachometer.....	43
Figure 32. Anemometer	44
Figure 33. Temperature humidity meter	45
Figure 34. Clamp ampere meter.....	46
Figure 35. Cylinder pressure vs. crank angle for three different inlet temperatures ...	48
Figure 36: Maximum cylinder pressure vs. engine speed for three inlet temperatures	50
Figure 37. Maximum pressure riase rate vs. engine speed for three different inlet temperatures.....	51
Figure 38: Heat release rate vs. crank angle at speed = 1800 RPM	52
Figure 39: Heat release rate vs. crank angle at speed = 1600 RPM	53
Figure 40: Heat release rate vs. crank angle at speed = 2000 RPM	53
Figure 41: Maximum cylinder pressure vs. engine load for three inlet temperatures .	54
Figure 42: Maximum pressure rise rate vs. engine load for three different inlet temperatures.....	55
Figure 43: Heat release vs. crank angle at load = 1.5 N.m for three different inlet temperatures.....	56

Figure 44: Heat release vs. crank angle at engine load = 3.9 N.m for three different inlet temperatures	57
Figure 45: Heat release vs. crank angle at engine load = 5.1 N.m for three different inlet temperatures	57
Figure 46: Air-to-fuel ratio vs. engine speed for three inlet temperature	58
Figure 47: Volumetric efficiency vs. engine speed for different inlet temperatures ...	59
Figure 48: Brake specific fuel consumption vs. engine speed at different inlet temperatures	60
Figure 49: Gained power vs. engine speed while running at T1 and T2	63
Figure 50: Gained energy vs. engine speed while running at T1 and T2	65
Figure 51: Air-to-Fuel ratio vs. engine load for three different inlet temperatures	66
Figure 52: Volumetric efficiency vs. engine load at three different inlet temperatures	67
Figure 53: BSFC vs. engine load for three different inlet temperatures	68
Figure 54: Gained power vs. engine load while running at T1 and T2	70
Figure 55: Gained energy vs. engine load while running at T1 and T2.....	72
Figure 56: NO _x vs. engine speed for three inlet temperatures	73
Figure 57: Hydrocarbon vs. engine speed for three different inlet temperatures	74
Figure 58: CO ₂ vs. engine speed for three different inlet temperatures.....	75
Figure 59: Smoke emission vs. engine speed for three different inlet temperatures ...	76
Figure 60: NO _x vs. engine load at three different inlet temperatures.....	77
Figure 61: HC vs. engine load for three different inlet temperatures	78
Figure 62: CO ₂ emissions vs. engine load for three different inlet temperatures	79
Figure 63: Opacity vs. engine load for three different inlet temperatures	80

CHAPTER 1: INTRODUCTION

This chapter aims to provide an overview about the selected topic by giving quick detailed information followed by presenting the motivation behind this research, the main objectives of this thesis project and finally summarizes the experimental methodology conducted.

1.1 Background

In light of other studies, there are several factors that affect the diesel engine performance characteristics (i.e. air-fuel mixing rate, volumetric efficiency and brake specific fuel consumption), combustion characteristics (i.e. in-cylinder peak pressure, maximum pressure rise rate and heat release) and emissions (i.e. NO_x, hydrocarbon, CO, CO₂ and smoke). One of the ways to improve those parameters is lowering inlet air temperature drawn into the engine [1]. Section 1.1.1 gives an overview about the effect of the ambient conditions on internal combustion engines. While section 1.1.2, illustrates the approaches adapted to control air inlet temperature.

1.1.1 Effect of ambient conditions on diesel engines

Extreme weather conditions in terms of high temperatures and relative humidity do not exist in all regions around the globe. However, Arabian Gulf tends to be sunny, hot and humid mostly through the year. According to weather and climate [2], the hottest months in Qatar ranges from June to August where the average maximum temperature ranges between 40°C – 45°C with an average maximum relative humidity that reaches up to 45% in July. July has been selected as the reference condition at which the test rig for this thesis project shall operate at.

Such extreme conditions affect the performance of the diesel engines in different aspects. High humidity will increase the probability for the engine to misfire as well as delaying combustion. On the other hand, as inlet temperature increases, volumetric efficiency decreases and eventually lowering combustion and engine efficiency [3]. Therefore, many researchers have studied the effect of ambient conditions on internal combustion engines especially supercharged and turbocharged diesel engines.

1.1.2 Approaches for controlling inlet air temperatures into ICE

Many researches have investigated many approaches to lower air inlet temperature drawn into the ICE of vehicles. Such approaches can be either to equip supercharged/turbocharged engines with an air-water intermediate heat exchanger just after the conventional intercooler to relatively lower the air temperature or introducing an intercooler coupled to the evaporator of the vehicle's AC in addition to a pump for circulations. These approaches will be discussed more deeply in chapter 2.

1.2 Motivation behind the project

Due to the fact that hot weathers are widely spread in Arabian Gulf region and especially in Qatar, this project focuses on offering a practical solution that aims to improve naturally aspirated diesel engine's efficiency by lowering air inlet temperatures through modifying vehicle's existing air conditioning system. Most of the recent studies focuses on introducing new parts into the vehicle; however, the solution offered by this project will save cost, eliminate introducing additional equipment and utilize existing vehicle's system without presenting complex modifications.

1.3 Research Objectives

The aim of the project is to study the effect of running a diesel engine at different controlled inlet air temperatures and observe the impact on engine's performance and emissions. The following are the main objectives of this project:

- 1) To develop a manually controlled air conditioning compartment that simulates the reference case in this thesis project (i.e. July's ambient parameters in Qatar)
- 2) To develop a new design of an air-cooled induction manifold which can be applied in real vehicles.
- 3) To diagnose the effect of running at different inlet temperatures on engine's performance, combustion and emissions characteristics.

1.4 Research methodology

This research is based on inducing different controlled air temperatures into the engine at a constant absolute humidity in order to investigate and analyze the performance and emission aspects of the targeted diesel engine. Specific devices have been used for sensing and others for measuring emissions such as smoke meter and gas analyzer. Moreover, an oscilloscope has been configured to the test bed via a pressure transducer, to measure pressure values inside the cylinder which generates waves that are used for further analysis using calibration equations.

Afterwards, a compartment was collectively designed and fabricated to condition the induced air into the engine with a defined temperature and relative humidity ($T_3=45^{\circ}\text{C}$ and $\text{RH}=45\%$) as a first step. This is due to the fact that the experimental works are done

inside a laboratory at approximately 22°C. Then, the drawn air passes through a cooling coil which is coupled to the evaporator of a water cooler that is controlled by an embedded thermostat inside the inlet manifold to achieve two different temperatures; T1=25°C and T2=20°C. All air parameters are monitored by temperature humidity meters.

Once the test-rig is ready with all controlled factors and measuring devices, the experiment can be initiated. The overall experiment has been divided into two main sections; running at constant load while varying the engine speed and vice versa with 5 steps each as illustrated in Tables 1 and 2.

Table 1. Section1 for data acquisition

Engine Speed (RPM)	Engine Load (N.m)
Constant speed at 1600	0.3
	1.5
	2.7
	3.9
	5.1

Table 2. Section 2 for data acquisition

Engine Speed (RPM)	Engine Load (N.m)
1400	Constant load at 1.5
1600	
1800	
2000	
2200	

All parameters have been measured on spot at each step including; engine performance, combustion and emissions characteristics. The analysis will compare all inlet temperatures based on the final plots and discussions. At the end, a clear conclusion has been deduced after all aspects and analysis have been presented for each case. Figure 1 shows the summary of research methodology in steps.

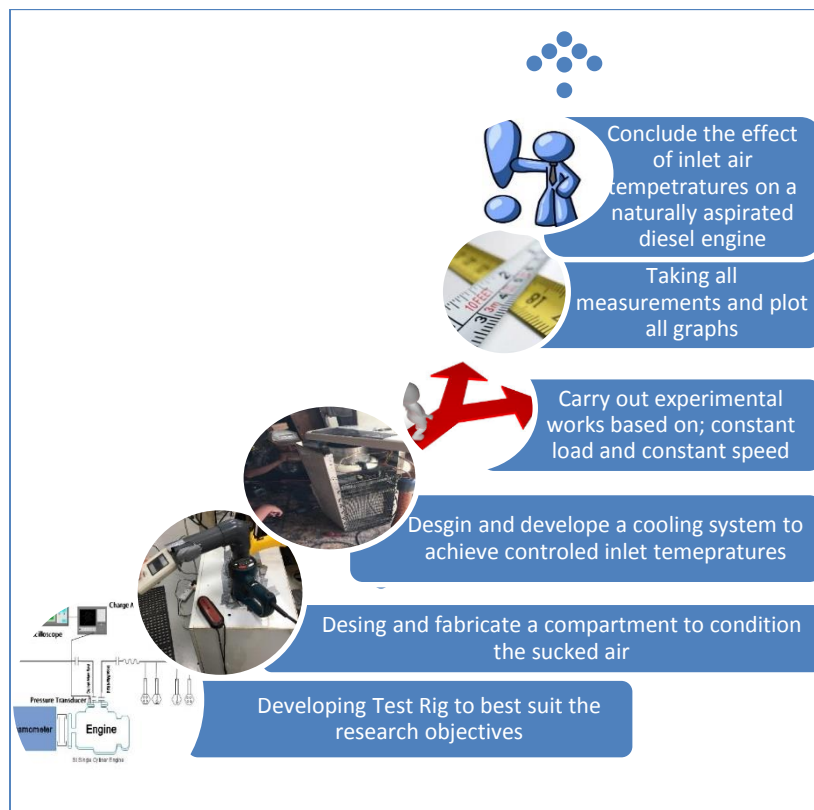


Figure 1. Research methodology steps

1.5 Thesis structure

- Chapter 1: Introduction

This chapter gives a brief background about the topic followed by detailed information about the selected strategy and presents different approaches to enhance engine's different characteristics. Then it presents the motivation behind this research, the main objectives and finally the experimental methodology.

- Chapter 2: Literature Review

This chapter discusses initially the main engine performance parameters followed by the effect of ambient air conditions on internal combustion engines. After that recent related experimental studies are illustrated with the outcomes that best fit the design of this thesis project. Finally, the outcomes of this chapter are listed in bulletin points.

- Chapter 3: Experimental setup

This chapter gives detailed explanation about the tool utilized explaining the various components and designs that finally result in a well-designed test rig followed by information about the sensing and measuring devices utilized to reach the objectives.

- Chapter 4: Results and Discussions

This chapter starts with the uncertainty Table of the calculated parameters followed by listing all engine's characteristics and selected parameters. All results were discussed and elaborated with validating via citation of recent studies.

- Chapter 5: Conclusion

This chapter summarizes the outcomes of this project in line with the listed objectives in a quantitative approach.

CHAPTER 2: LITERATURE REVIEW

This chapter of the report will go through the detailed literature review described in the introduction. Section 2.1 starts by giving details about the Diesel engines and recognizing their importance in all types of industries now a days. Followed by Section 2.2 that discusses the engine performance characteristics (i.e. engine power, break specific fuel consumption and Break mean effective pressure). Then Section 2.3 gives a review about the effect of ambient conditions (in QATAR) including humidity and air temperature on engine performance, engine volumetric efficiency as well as emissions. Moreover, detailed discussion on the working mechanism of A/C in vehicles will be presented in Section 2.4 and how such systems may affect engine performance while in Section 2.5, related experimental methods for other researchers will be discussed in depth in light of enhancing induced ambient conditions in internal combustion engines. In Section 2.6, other strategies to enhance engine parameters will be discussed briefly. Finally the outcomes of the literature chapter will be presented in Section 2.7.

2.1 Diesel engine

Diesel engines were traditionally been underestimated in terms of power and class. They were limited to be utilized in trucks, ambulances, taxis and vans. After improving the injection system and became more sophisticated, there were almost 65,000 diesel cars sold in 1985 in UK compared with only 5,380 in 1980 [4]. The main advantages of Diesel engines over gasoline engines is their lower running cost which is due to the fact that diesel engines acquire greater efficiency due to their higher compression ratios (12-24) [3]. Diesel prices stand a crucial factor in running diesel engines; hence, diesel prices in Qatar to be

specific, is relatively lower than the gasoline prices [5]. As a result, a chance in utilizing diesel-powered vehicles.

2.2 Engine performance characteristics

Engine performance can be characterized through several parameters. In order to develop internal combustion engine, all the affecting parameters shall be taken into consideration to fulfill governmental regulations in terms of emissions and to have an overall comparable engine efficiency.

2.2.1 Engine power

There are two common terminologies that defines engine power; maximum rated power and normal rated power. Maximum rated power refers to the highest power that an engine is allowed to achieve for short periods of time. Moreover, normal rated power refer to the highest power developed in continuous operation [4]. The net power output depends on the size and design of the engine keeping in mind the running speed and the load it encounters. It can be expressed in kilowatts or horsepower. There is another important terminologies that best describe engine power; indicated and brake power [3].

Indicated power is the power achieved by converting chemical energy into mechanical energy via combustion of the fuel inside the cylinder without considering the power loss in the mechanical components due to friction. While brake power is the net power achieved at the wheels including all losses. Therefore, mechanical efficiency is considered to be the ratio of brake power to the indicated power as per equation 1:

$$\text{Mechanical Efficiency} = \frac{P_b}{P_i} \dots \dots \dots \text{Equation (1)}$$

Where, P_b : brake power and P_i : indicated power

2.2.2 Brake Specific Fuel Consumption (BSFC)

BSFC, is the rate of the fuel consumed relative to brake power produced; hence, it is another way to measure the efficiency of the engine. Figure 2 shows the effect of air inlet temperatures with BSFC as per the experimental findings by Saber [4].

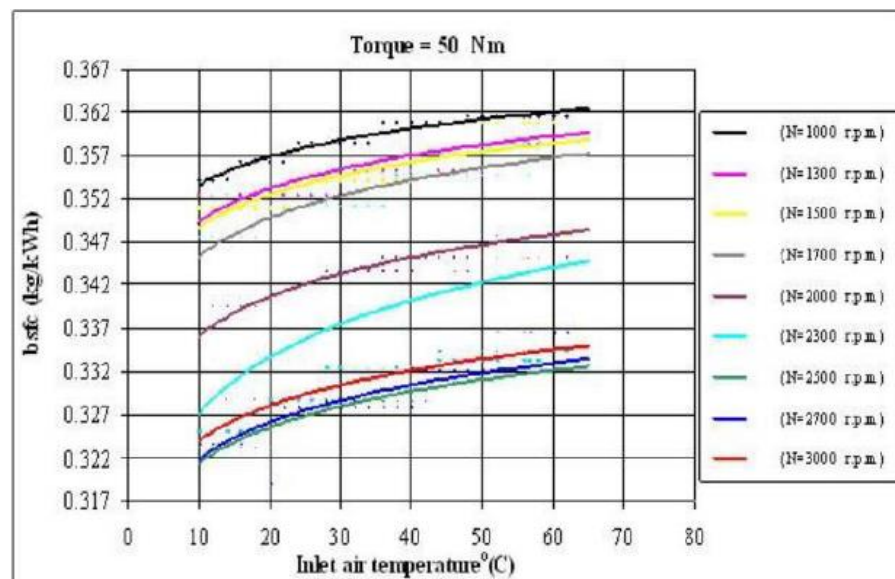


Figure 2. Effect of inlet air temperature on fuel consumption [4]

2.2.3 Break Mean Effective Pressure (BMEP)

Another engine performance measure is called mean effective pressure (MEP). It is purely theoretical and does not represent the actual cylinder pressure. It addresses some comparison measures between engines at rated parameters and others. It can be obtained by dividing the work per cycle by the displaced volume of the cylinder.

$$mep = \frac{P \cdot n_r}{V_d \cdot N} \dots\dots\dots \text{Equation (2)}$$

P: Pressure (kPa)

n_r : Number of crank revolutions relative to power stroke per cylinder

V_d : Displaced volume of cylinder (m^3)

N: Number of revolution (rev/min)

Maximum brake mean effective pressure of typical engine designs is well established and tabulated; therefore, actual bmep of any engine can be compared with this norm. As an instance, naturally aspirated four-stroke diesel engines, maximum bmep is in the range of 700 to 900 kPa. [4]

2.3 Effect of Ambient conditions on ICEs (QATAR CLIMATE)

Arabian Gulf climate and Qatar to be specific is well known with its hot and humid weather during most of the months. The most critical ambient conditions that highly affect engine performance are; ambient air temperature and relative humidity. Hence, inlet temperature has major effect on volumetric efficiency of the engine as will be discussed over the following sections.

2.3.1 Humidity

Humidity is the amount of water vapor exist in air. As humidity increases, the engine will have more probability to misfire; hence, delay in combustion. On the other hand, lower humidity levels can affect the knocking margin as well as NO_x emissions; however, lower engine efficiency [6]. Figure 3 describe the effect of humidity on engine efficiency; hence, the higher the humidity, the lower the efficiency and NO_x level.

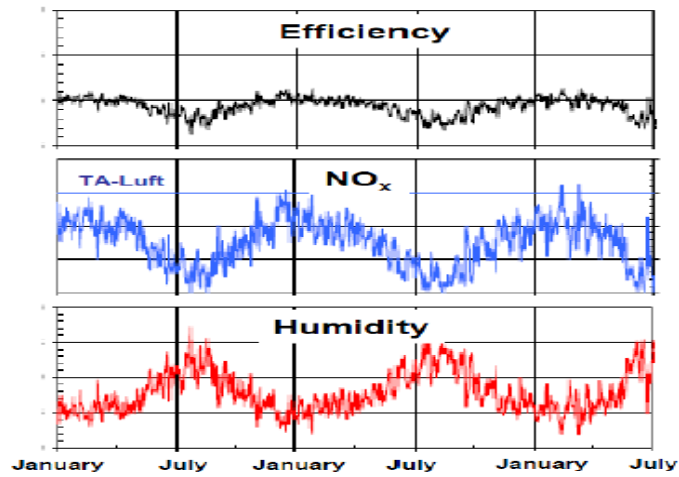


Figure 3. Effect of humidity on engine efficiency and NO_x level [6]

2.3.2 Inlet Air Temperature

The temperature that is measured outside the engine compartment coming to the cylinder is called ambient inlet air temperature; hence, does not have direct effect on the engine efficiency, it affects the volumetric efficiency of the engine. Furthermore, starting from April up to November, warmest temperatures are illustrated, refer to below Figure 4 [7].

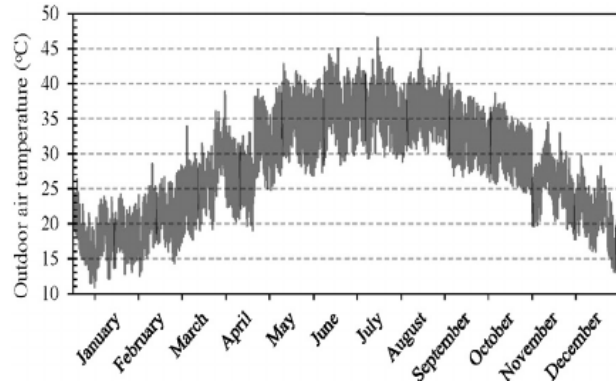


Figure 4. Annual average temperature distribution in Qatar [7]

With reference to Figure 4, the higher the temperature, meaning the lighter the air being sucked into the engine which results in lower combustion efficiency [6]. Therefore, it is recommended that relatively low inlet temperature should be used to gain more volumetric efficiency; hence, higher combustion efficiency as described in Figure 5.

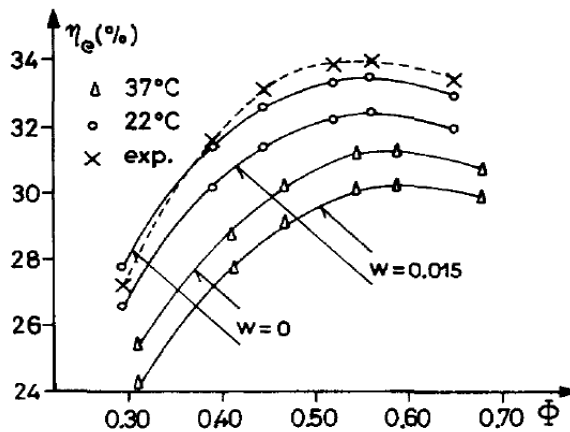


Figure 5. Combustion efficiency against different ambient temperature and humidity [6]

2.3.3 Volumetric Efficiency Improvements

Volumetric efficiency is a ratio of the mass of air and fuel that comprises the cylinder medium divided by the mass that would occupy the displaced volume. The denser the air sucked to the engine, meaning more air to fuel ratio that will be utilized during combustion; hence, more power [3]. There are many ways to enhance the volumetric efficiency such as; using turbos or superchargers. As a result of forced induction volumetric efficiency can exceed 100% [8]. Other way is by cooling the inlet ambient temperature using mini separate HVAC system or any AC modified systems which will be illustrated and discussed in details in the coming sections.

2.4 Air conditioning system in cars

The core of this research is to illustrate the effect of inlet ambient conditions on engine performance. Therefore, general understanding of A/C system in cars will give clearer image of how such system can be utilized for enhancing inlet air condition.

2.4.1 How does it work?

All air conditioning systems work similarly; whether they are utilized in buildings, fridge or oven civilian cars for cooling or heating purposes. It is a fact that in order to remove/add heat and moisture, energy is being consumed. Therefore, turning the AC in cars actually result in consuming diesel/ gasoline from the cars' tank due to the extra work done on the car's engine [9]. Hence, if the same AC unit is being modified and utilized to cool the inlet temperature coming to the engine compartment, this will result in more power which eventually outweigh utilizing existing A/C inside the vehicle.

Controlling heat transfer efficiently between two regions of different temperatures

requires special cyclic devices. Refrigerators (for cooling objectives), heat pump (for heating objectives) are the most well-known devices in modern times. Those devices operate by a cycle called vapor compression refrigeration cycle. The main components of the cycle as shown in Figure 6 are; compressor, condenser, throttling valve and evaporator [10].

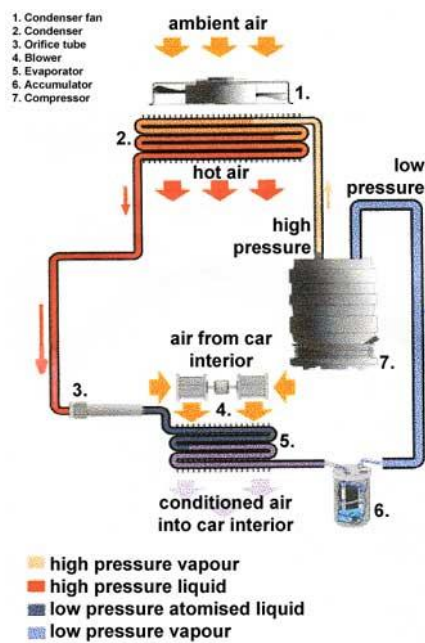


Figure 6. Schematic shows the components of vapor compression cycle [10]

In order to calculate the amount of heat gain at the evaporator, heat loss at the condenser and the amount of work input at the compressor the enthalpies at each stage must be determined. Eventually the coefficient of performance (COP) of the cooling system can be calculated which gives an indication of the reliability of the air conditioner.

$$COP_C = \text{Cooling load} / \text{Work input into the compressor} = Q_L / W_{in} \dots \dots \dots \text{Equation (3)}$$

2.4.2 Intercooling concepts and effects

Intercooler is a device used to cool the intake air coming to the engine compartment when using supercharged or turbocharged engine. It is a way to increase the volumetric efficiency as discussed earlier; hence, intercoolers can be either Air-to-Air or Air-to-Water [11].

Turbocharger/supercharger compresses the air and raises its temperature very quickly. As a result, its density drops; therefore, increasing the density of air by cooling allows higher air to fuel ratio coming towards the engine cylinder, thus giving more power [3].

2.4.2.1 Air-to-Air intercooler

It utilizes air from the atmosphere at very high speed to cool down the fins of the intercooler which consequently lowers the temperature of the compressed air coming from the turbo/supercharger through its network of tubes as shown in Figure 7 [11]

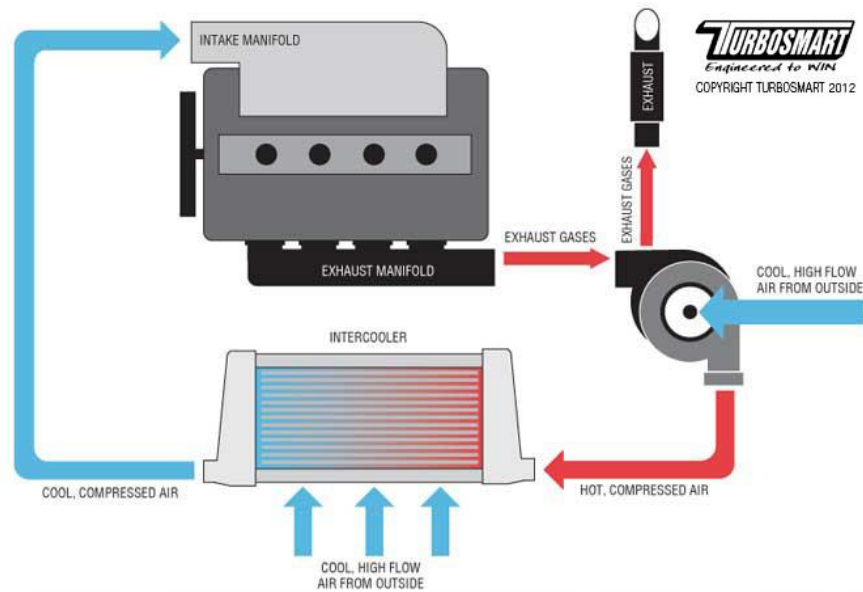


Figure 7. Schematic of Air-to-Air Intercooler [11]

2.4.2.2 Air-to-water intercooler

This system utilizes water to cool down the temperature of the compressed air coming from the turbocharger/supercharger. Initially, water is being pumped into the intercooler and sucks heat from the compressed air. Afterwards, the heated water is then pumped back through a radiator via different circuit and the cooled compressed air is pushed into the cylinder as illustrated in Figure 8 [11].

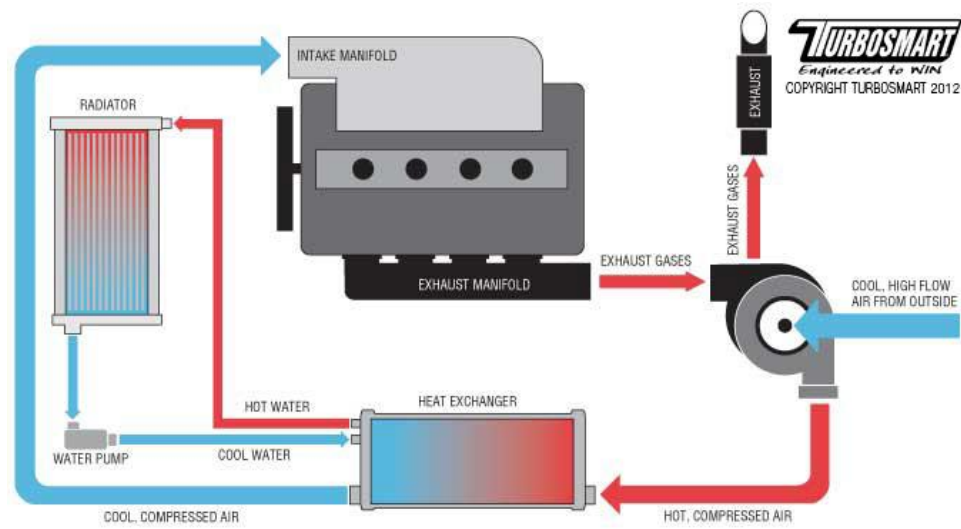


Figure 8. Schematic of Water-to-Air Intercooler [11]

2.5 Experimental test rigs for ICEs

The intention of setting up experiments is to examine the concept of intercooling/specific ambient conditions with minim efforts in parts without imposing any big improvements to the concerned engine/vehicle. Many scientists and researchers have conducted experiments that manipulated the ambient temperature/humidity. It was found that artificially controlling the ambient conditions to be energetically vital and effective in the sense of cooling the intake air whether the engine is naturally aspirated or equipped with supercharged/turbocharger. This thesis project will utilize a cooling method inline to pre-found results that will be briefly discussed in the coming paragraphs.

In 1996, Cherng-Yaun et al [12] conducted an experiment on a direct injection marine diesel engine of four cylinders arranged inline as described in below Table 3:

Table 3. Specifications of marine diesel engine [12]

Item	Specifications
Type	4-Stroke, L-4 Marine, water-cooled, direct-injection
Displacement volume	3,856 cc
Cylinder bore x stroke	4-102 x 118 mm
Max. horsepower	88/2,800 (PS/rpm)
Compression raio	17:01
Min. idle speed	550 rpm
Air admitting	Naturally aspirated
Injection angle	13 degree BTDC

Charge air is forced into the intake manifold via a blower directed through an air conditioner at which air properties changes (i.e. temperature and relative humidity). The specifications of the A/C unit are listed in Table 4.

Table 4. External A/C system specifications [12]

Item	Specifications
Cooling capacity	15760 Btu/hr (x2)
Heating capacity	9 kw
Humidity capacity	22 kg/hr (Coil-type humidifier) 2.4 kg/hr (x2) (Ultrasonic humidifier)
Air-inlet	Naturally aspirated
Temperature range	From 10 to 50 °C
Humidity range	From RH 10% to RH 95%

Set up matrix is summarized in Figure 9 where data acquisition system along with engine cycle analysis software were utilized to ease acquiring data. The computerized

laboratory is located in a coastal region to simulate real marine environment.

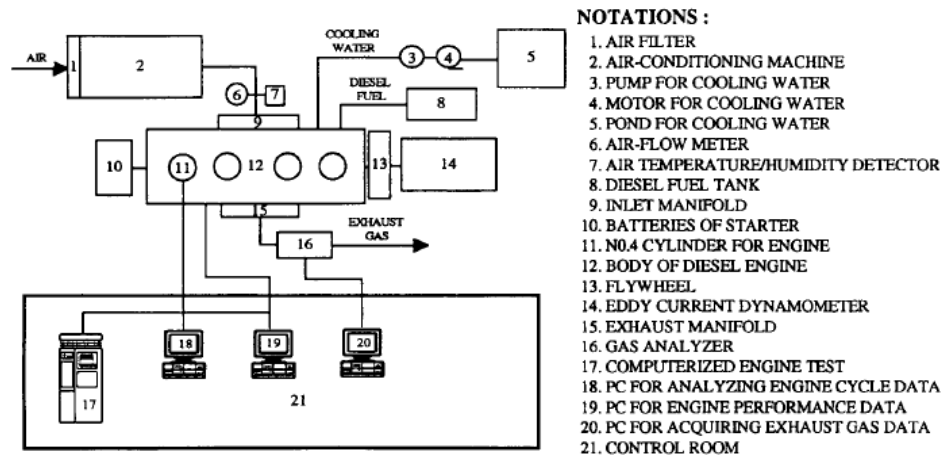


Figure 9. Schematic of experimental apparatus

It was concluded that engine performance and exhaust characteristics are highly effected by charge air temperatures rather than air humidity. Moreover, it was observed that BSFC, carbon monoxide and sulfur dioxide have increased while brake torque has decreased with the increase of charge air temperature. Meanwhile, this thesis project focuses on enhancing the ambient conditions introduced into automobiles by utilizing existing A/C system.

Hsu in 2002 [13] studied the effect of having different manifold air temperature (MAT) on a turbocharged direct injected diesel engine in terms of engine performance and combustion characteristics. Table 5 shows the detailed outcome of such variation on a diesel engine.

Table 5. Effect of different inlet temperatures on diesel engine performance [13]

<u>Inlet Manifold Air Temperature (°C)</u>	85	70	55
SFC (kg/kWh)	0.1966	0.1918	0.1891
Pmax (MPa)	15.51	15.79	15.84
Smoke (Bosch #)	0.3	0.26	0.2
MAT Density (kg/M³)	3.23	3.39	3.56
Trapped Air/Fuel Ratio	27.8	29.2	31.9
Ignition Delay (ca)	5.3	5.6	6.1
Fuel Burned in Kinetic Stage (%)	3.9	5.4	6.9
Relative Cycle Efficiency (%)	93.2	93.9	94.1

Moreover, Figure 10 explains the data stipulated above in light of peak pressure differences inside the cylinder against crank angle degrees.

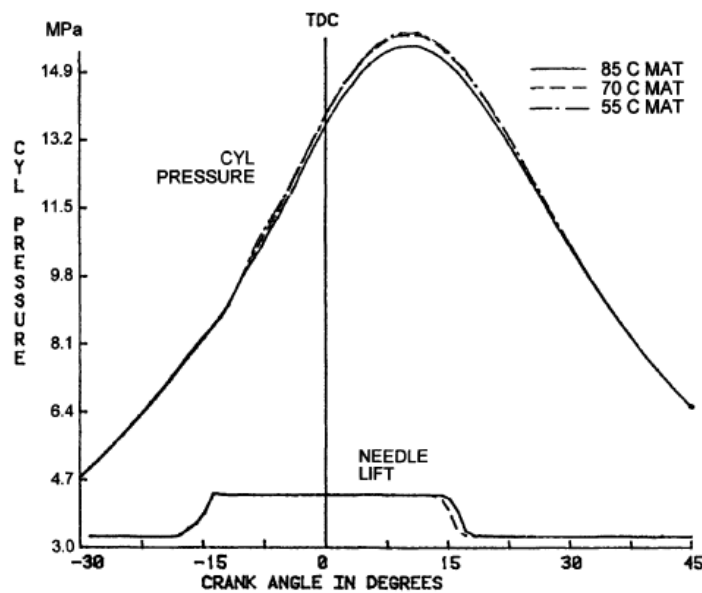


Figure 10. Cylinder pressure variation of three different inlet temperatures [13]

In 2014, Kadunic et al [14] targeted a turbocharger SI engine for passenger cars as illustrated in Table 6 by modifying its existing air conditioning system; however, two experimental set ups were designed to study deeply the effect of the properties of charge intake air to engine performance. Set up one is illustrated in Figure 11 which consists of two heat exchangers. The first one is a conventional water-to-air intercooler that cools the intake air to not more than 40°C then undergoes further cooling by the extra intercooler ICE as shown on the same Figure below. It utilizes existing parts of A/C system in the car to absorb the heat from the fluid that exchanges heat with the evaporator. However, extra components were introduced into the vehicle which increased, cost, complexity and weight.

Table 6. Turbocharged SI Test engine [14]

Test engine data
Spark ignition, homogenous direct injection, Turbo charged
4 Cylinders inline, DOHC 16 valve
Displacement: 1390 cm³
Nominal output: 90 kW
Peak torque: 200 Nm
Nominal output from 5,000 to 5,500 min⁻¹

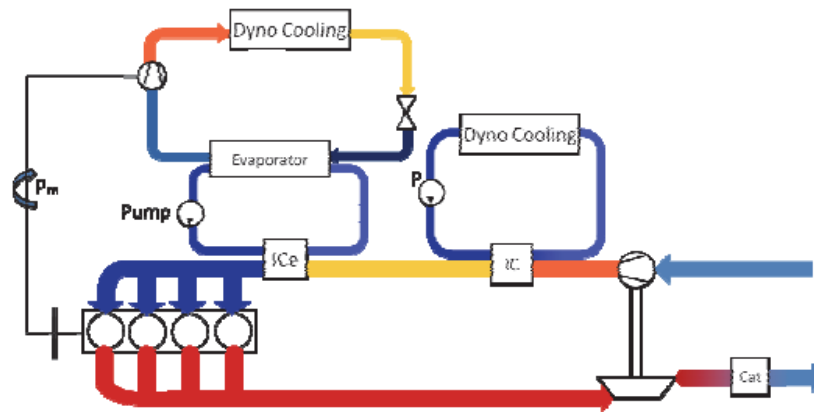


Figure 11. Test Setup 1 consisting of two heat exchangers [14]

Set up two shows an improved system by eliminating the cold fluid circuit as shown in Figure 12. It directly linked the intercooler outlet air with the evaporator of the A/C system (ICev). The main advantage of this setup is reducing the costs of weight, additional parts/accessories and space. Eventually, increasing the efficiency of the cooling system by eliminating the losses due to the lining of the extra heat exchanger.

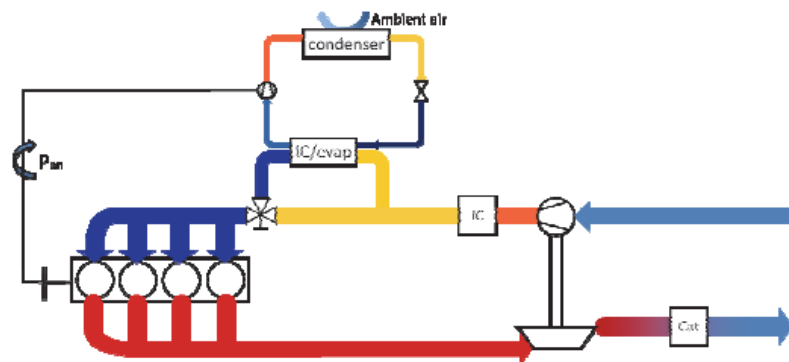


Figure 12. Test setup 2 with improved intercooler/evaporator system [14]

Finally, the first setup showed that modified A/C systems can improve engine's efficiency up to 9%; however, the second test setup was not experimented, but the author wanted to show that there are promising potential in upcoming automobile market through modifying existing passenger cars without having to redevelop new cars. Further exploration for Test setup 2 has been conducted in this project thesis.

In 2015, Abdullah et al [15] conducted an experiment on a naturally aspirated gasoline engine at which three different manifold air temperatures were charged into the engine to investigate their effect on fuel consumption and emissions. The engine's specifications are shown in below Table 7 while the engine's setup is shown in Figure 13

Table 7. Gasoline engine's specifications [15]

Power train engine and performance	
Engine	4 Cylinder, DOHC 16V
Maximum speed (km/h)	190
Acceleration 0-100km/h	10.5
Fuel	Gasoline
Injection type	Fuel system multi-point injection (MPI)
Number of cylinder and configuration	4 (in-line)
Displacement (cm³)	1597
Bore (mm)	76
Stroke (mm)	88
Compression ratio	10:01
Maximum power (kW/RPM)	6,500 @ 125 HP (93 HP)
Maximum torque (Nm/RPM)	4,500 @ 150 Nm

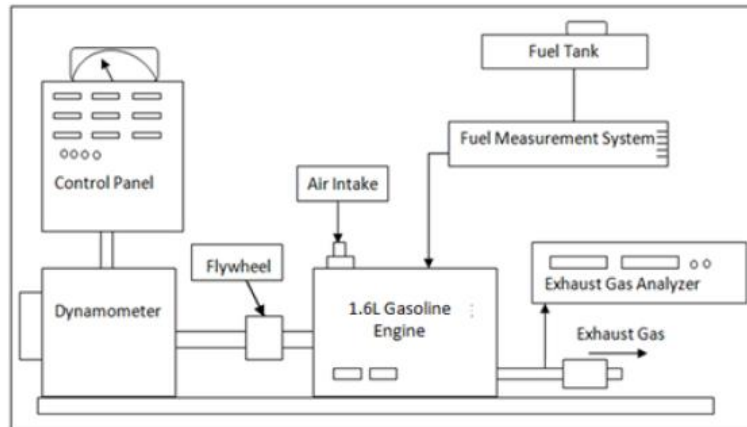


Figure 13. Detailed schematic diagram of the engine's setup [15]

The results showed an improvement in fuel economy with lowering inlet air at which the lowest value for brake specific fuel consumption occurred at air intake of 20°C temperature. Moreover, fuel emissions such as carbon monoxide and unburned hydrocarbons decreased when lowering charged air temperatures. While in this thesis project, the target is to examine passenger vehicles that are naturally aspirated diesel engine and utilizing existing air conditioning system.

In 2017, Yan Chang et al [16] investigated the effect of ambient humidity and temperature on spark assisted compression ignition engine as characterized in Table 8 in terms of combustion characteristics. The experiment was conducted at different three inlet air temperatures and constant absolute humidity. It was observed that the heat release rate is directly proportional to air ambient temperature unlike in diesel engines as shown in Figure 14.

Table 8. Spark assisted compression ignition engine specifications [16]

Engine specifications	
Displacement volume (L)	2
Number of cylinders	4
Bore (mm)	86
Stroke (mm)	86
Connecting rod length (mm)	145
Compression ratio	11.7:1
Injection type	Direct (spray guided)
Turbocharger	Borg Warner K04 twin scroll

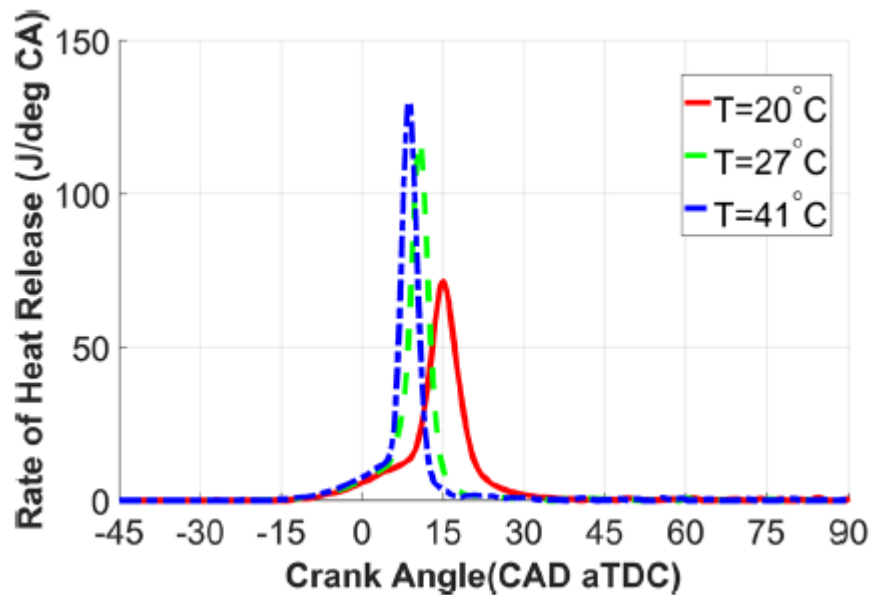


Figure 14. Effect of inlet air temperature on rate of heat release [16]

This study proves that the effect of changing inlet air temperatures drawn into internal combustion engines does not necessarily retain same results as it is linked to the types of engine being utilized (i.e. CIE, SIE, etc...)

2.6 Inlet Manifolds

Previous chapters were discussing the importance of lowering the temperature and humidity of the drawn intake air in improving engine performance and lowering emissions. This chapter will discuss briefly about another factor that would enhance effectively engine performance through generating a swirl inside the cylinder to improve air to fuel mixture.

Mergary et al in 1990 [17] found out that volumetric efficiency and air flow rate towards the cylinder are directly proportional to the fixed length of the intake duct at a speed of 1000-3000 rpm. Nowadays new technology has been introduced which is using the variable length induction manifold. When high rpm is needed, shorted length induction manifold is utilized while for low rpm and high torque, longer length induction manifold to be used.

Three major intake manifold designs are always under intensive studies; spiral, helical and helical-spiral manifold designs. Moreover, the interested output is always related to higher swirl intensity which will result in higher volumetric efficiency. With reference to many researches, the use of helical-spiral manifold design results in improving the engine efficiency and lowers exhaust emissions compared to the other manifold designs. [18]

2.7 Outcomes of the Literature reviews

- Lowering inlet air temperatures drawn into compression ignition engines result in better engine performance and emissions. Unlike, running the same in other types of internal combustion engines.
- All recent studies have introduced additional equipment and modifications into the

engines which has adverse effect on space, cost and effort.

- Passenger vehicles were not the focus of the author's study, most of the researches were carried on industrial engines.
- Most of the recent studies conducted their experiments on turbocharged engines unlike the focus of this thesis project.
- There are other strategies to enhance internal combustion engine's performance, combustion and emission characteristics.
- This thesis project, eliminate adding extra equipment and complex modification into a passenger's naturally aspirated diesel engines. Vehicle's existing air conditioning system will be utilized with minor modifications to cool down the air drawn onto the engine with feedback system.

CHAPTER 3: EXPERIMENTAL SETUP

This chapter will give a detailed information about the experimental tool in section 3.1 and the devices that were used for measurements during the experimental works in section 3.2. Finally, in section 3.3, safety rules and regulations during the experimental work will be discussed.

3.1 Experimental Method

The experimental tool utilized in this project is a single cylinder, four stroke and naturally aspirated diesel engine that is characterized in Table 9. Figure 15 shows the engine test bid and the measuring tools utilized in this project.

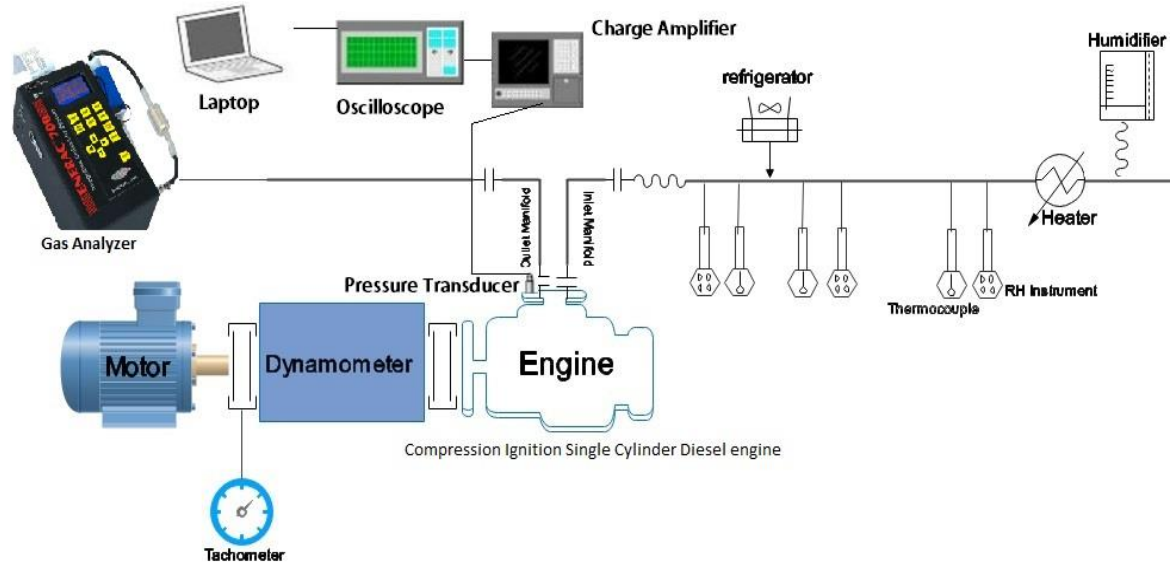


Figure 15. Schematic of Test Rig

Table 9. Specification of diesel engine test bed

Parameter	Specification
Number of Cylinders	Single cylinder, 4-stroke
Engine Type	Compression ignition engine
Nature of cooling	Water-Cooled Engine
Bore (m)	0.082
Stroke (m)	0.068
Capacity, cc/	359.1
Compression Ratio, r_c	18
Maximum speed, rpm	3200
Max. Power (H.P.)	6.5
Used Fuel	Diesel
Inlet valve opens, deg	8 BTDC
Inlet valve closes, deg	223 ABDC
Exhaust valve opens, deg	40 BBDC
Exhaust valve closes, deg	37 ATDC
Injection timing, deg	(29 BTDC-4BTDC)

Dynamometer was coupled to the motor via coupling and controlled by a switch positioned at the top of the engine. Figure 16 illustrates the mechanism of coupling between the motor and the dynamometer and finally to the engine. Moreover, the revolution of the shaft can be detected using speed tachometer.

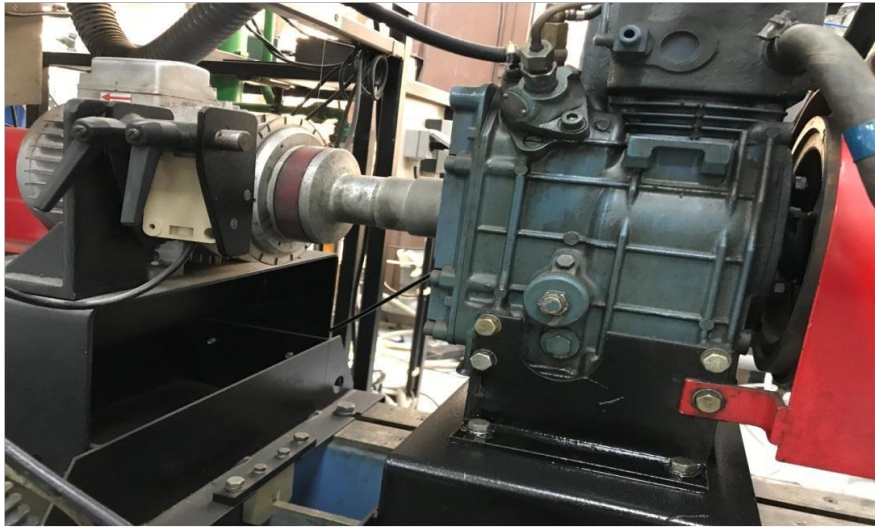


Figure 16: Dynamometer coupled to the crankshaft of the engine

Control board shown in Figure 17 governs all controlling features as shown below:

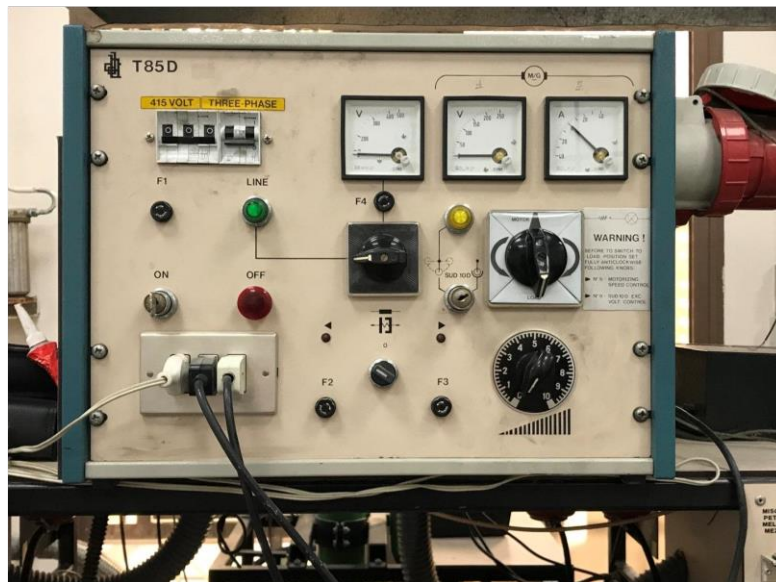


Figure 17: Control Board including all Main Switches

Figure 18 shows two vessels that are used for fuel supply to the engine however only Diesel fuel has been utilized in this project.

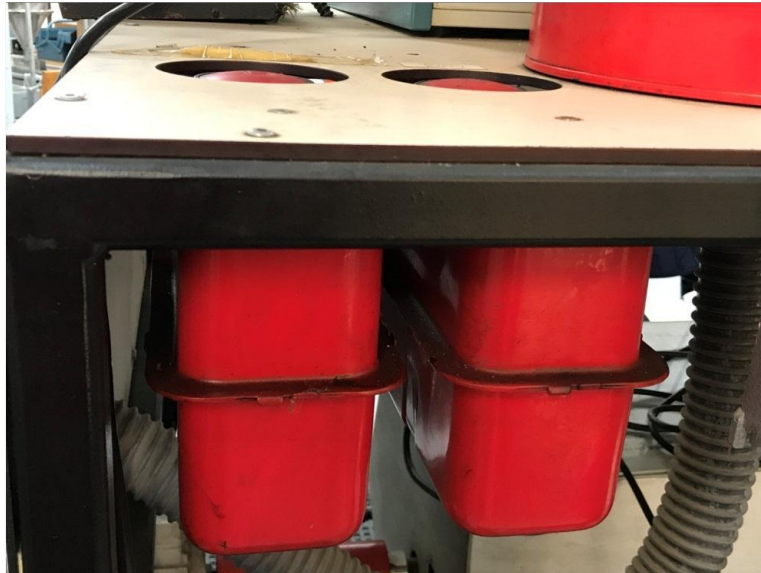


Figure 18. Fuel Tanks

Fuel consumption was measured using a calibrated burette and a stopwatch by adjusting the fuel supply valves for a constant fuel travel (i.e. five cubic centimeters) as illustrated in Figure 19 and 20.

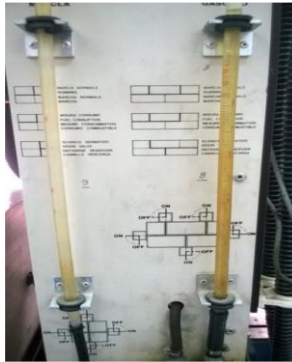


Figure 19. Fuel calibrated burette



Figure 20. Fuel supply valves

The experimental setup is located in well-equipped laboratory at Qatar University, hence running at a room temperature. Therefore, a compartment was initially designed to simulate the reference ambient conditions while maintaining the engine naturally aspirated. Engine's minimum volume flow rate of air is 200L/min without being coupled to any system. Table 10 shows the main specifications and components of the designed air conditioning compartment.

Table 10. Technical specifications of the air conditioning compartment

Components	Specifications	Advantage
Honeycomb paper	1.5" thick .75" cell and 20" length	Acting like water reservoir
Two Heat Guns	190 to 350L/min. flow rate - 50-550C Temperature range	Increasing air temperature – lower than minimum engine air flow rate
Sink	300cm X 150cm X 100cm	For containing water
Electric submersible pump	7.1 x 2.1 x 1.8 inches, AC, 8 Watts power output and 210 GPH	for circulating water across the honeycomb paper
Frame/compartment	400 X 200 X 150cm	Governing all components

Two heat guns were utilized at the same time to increase the air humidity and temperature inside the compartment prior starting the engine. Once the engine starts, one heat gun will be operational with minimum volume flow rate to ensure the engine is naturally aspirated. The compartment was punctured at the top with ½” hole to ensure air circulation inside the system at elevated engine’s speeds.

Figure 21 shows a detailed design cycle of the compartment. As the engine draws air from the compartment, air properties change and finally configured on trial and error basis depending on engine’s load and speed. Once the reference case is met, the drawn air passes through another design that cools air prior entering the engine. A water cooler has been utilized and coupled to a prefabricated copper coil embedded into the induction manifold of the engine where the outlet air from the coils coming to engine inlet is controlled via a thermostat. Table 11 shows the technical specifications of the cooling system followed by a detailed design cycle illustrated in Figure 22.

Table 11. Technical specifications of the cooling system

Description	Specifications
Refrigerant type	R-134A
Refrigerant minimum Temperature (°C)	-20
Power Consumption by water cooler compressor (Watts)	151.8
Size of cooling coil (diameter X length) in the induction manifold	1/4" x 15 meter
Range of air inlet temperature into the engine (°C) at reference case	16 - 35

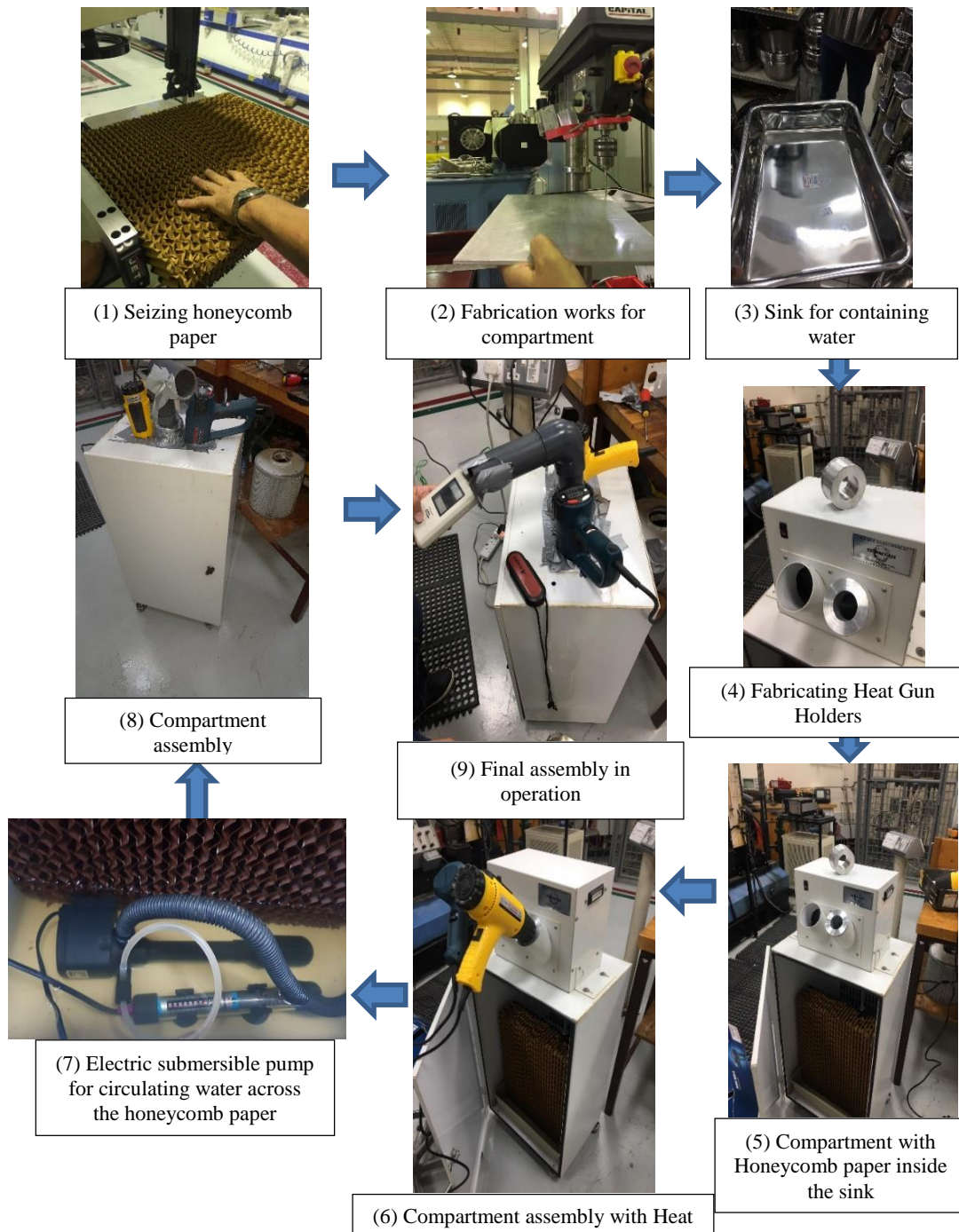


Figure 21. Air conditioning compartment

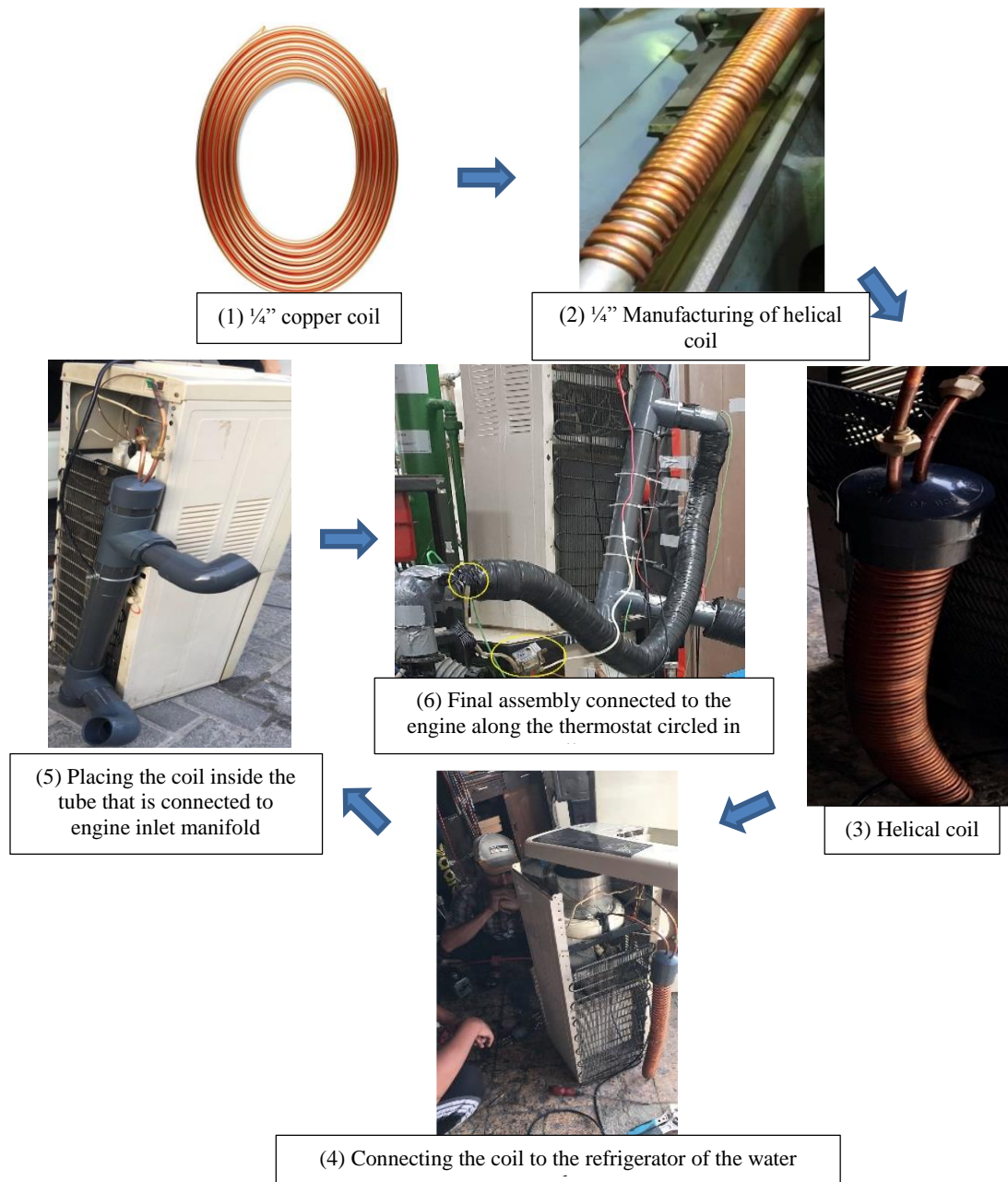


Figure 22. Design of an air cooled induction manifold

Furthermore, the in-cylinder pressure has been measured for further analysis and has been done by piezoelectric pressure transducer shaft encoder. Followed by oscilloscope which has been used to observe the output signals. Afterwards, Matlab software has been utilized to change the signals into pressure relative to crank angle. Through various coding, in-cylinder peak pressure, change in pressure with respected to crank angle and heat release through combustion can be obtained which best serve the project's objectives.

Once in-cylinder pressure is known, further analysis has been done on exhaust emissions to look into the impact of having different inlet air temperatures on the engine exhaust emissions. Therefore, different tools have been utilized to measure exhaust emissions and smoke opacity. The ENERAC Model 700 was utilized to measure exhaust emissions like CO₂, CO, NO_x and unburned hydrocarbons. Moreover, smoke meter (ECO SMOKE 100) has been used to detect smoke emissions for the same engine.

3.2 Measuring Devices

In order to have a well-integrated test rig, devices/tools have been utilized to keep the drawn air monitored and controlled at almost all locations through the system. This section provides the important features and specifications for the devices that have been used for data acquisition throughout the experiments. The first device that will be discussed is the oscilloscope followed by pressure transmitter, gas analyzer, smoke meter and finally speed tachometer.

3.2.1 The Oscilloscope

The oscilloscope utilized in this setup is GW-Instek (Model GDS-3152), as shown in Figure 23.



Figure 23. GW-Instek oscilloscope (Model GDS-3152)

Once the data are collected, they are displayed on its screen which can be saved later on for further analysis as shown in Figure 24.

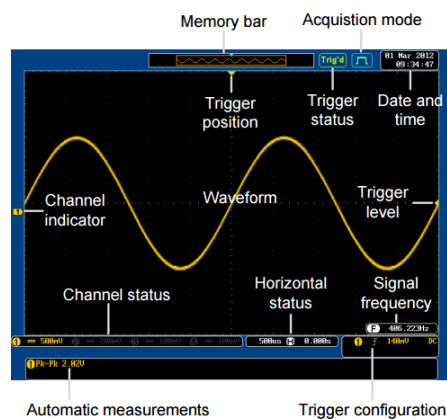


Figure 24. Waveform displayed on oscilloscope's screen

3.2.2 Pressure Transducer

The pressure transducer utilized in this project has a range of 7 bars. The response of output pressure for the sensor is 10 pC/psi. Figure 25 and 26 illustrates both; pressure transducer and charge converter.

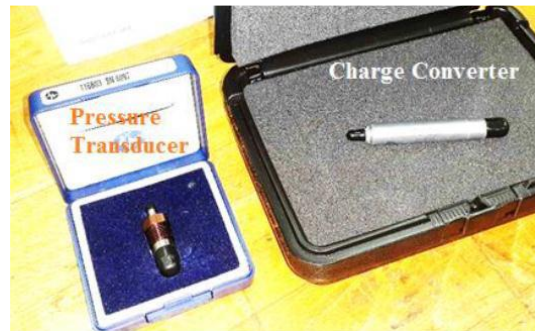


Figure 25. Pressure transducer and charge converter



Figure 26: Pressure transducer

3.2.2.2 Calibration Procedure

The same sensor was re-calibrated to check its healthiness even though it came with its calibration certificate attached in Appendix A. It was calibrated via the available facility

at Qatar University by connecting the sensor to the bench and compare its output signal to the provided chart as shown in Figure 27.

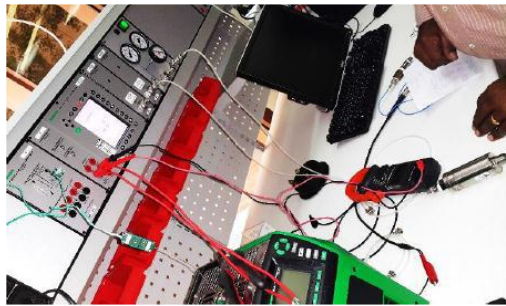


Figure 27. Pressure transducer calibration

3.2.3 Gas Analyzer

The ENERAC Model 700 Integrated Emissions System as shown in Figure 28 is designed to sense exhaust emissions. The Model 700 emissions analyzer remove, clean, finally dry the taken sample



Figure 28: ENERAC model 700 integrated emissions

Once the probe is inserted in the exhaust pipe of the engine, a pump will suck a sample which is then cleaned and dried before entering the system. ENERAC Model 700 Emissions system has large number of sensors that best serve the objective of this project. The following Table 12 shows the integrated sensors which will be utilized during the experiment to measure exhaust emissions along with their accuracy ranges:

Table 12. Gas Analyzer sensors and accuracy ranges

Sensor	Range	Accuracy
Carbon monoxide	0-2,000 PPM	2 PPM
	10,000/20,000 PPM	10 PPM
Nitric oxide	0-300 PPM	2 PPM
	2,000/4,000 PPM	5 PPM
Nitrogen dioxide	0-300 PPM	2 PPM
	1000 PPM	5 PPM
Sulfur dioxide	0-2,000 PPM	2 PPM
	6000 PPM	5 PPM
Oxygen	0-25%	0.2% of reading
Carbon dioxide	0.0%-16.0%	0.30%
	16.1%-20.0%	5% of reading

3.2.3.2 Calibration Procedure

Calibration of the system is recommended annually. Through which the device is sent to the factory for complete calibration depending on the sensor calibration span. Calibration for the same system was done on the 6th of January, 2018 in order to ensure accurate data and calibration certificate is attached on Appendix A

3.2.4 The Smoke Meter

Eco smoke 100 is the smoke meter utilized in this project to measure smoke emission. The unit comprises both; electronic & mechanical parts. Figures 29 and 30 depicts the utilized smoke meter and Table 13 shows the technical specifications and accuracy ranges of the device



Figure 29. Smoke meter overview



Figure 30. Smoke meter ports

Table 13: Technical Specifications of the Smoke Meter

Measurement Parameters	Range	Resolution	Condition
Opacity	0 - 99.9 %	0.10%	-
K-Value	0 - 9.99 m-1	0.01 m-1	-
Repeatability	± 0.1 m-1	-	-
Zero & Span drift	± 0.1 m-1	-	-
Response time-Physical	<0.4 sec	-	-
	< 1 milli.	-	-
Response time-Electrical	sec.	-	-
Warm up time	<7 min	-	25 C & above
Engine Oil temperature	0-150 C	1 C	-

3.2.5 Speed Tachometer

Testo 465 tachometer was utilized in this project to measure the engine speed (RPM). Figure 31 shows the speed tachometer. Table 14 shows the technical specifications of the device.



Figure 31. Speed tachometer

Table 14: Technical specifications of the speed tachometer

Parameter	Value
Measuring range	1 - 99999 rpm
Accuracy	$\pm 0.02\%$ of mv
	0.1 rpm (100 to 999.9 rpm), 1 rpm (10000 to 99999 rpm)

3.2.6 Anemometer

Kestrel 3000 Environmental Meter illustrated in Figure 32 was used in this experiment to measure the speed of the drawn air into the engine via an embedded electronic rotating vane. Moreover, Table 15 shows the specifications and accuracy ranges of the device.



Figure 32. Anemometer

Table 15: Technical specification of the anemometer

Specifications	Speed	Temperature	Relative Humidity
Operational Range	0.6m/s to 60m/s	-45.0°C to +125.0°C	0% to 100%
Accuracy		±1°C	±3%

3.2.7 Temperature Humidity Meter

It is a digital thermometer and hygrometer described in Figure 33 and stipulated in Table 16 used to measure temperatures for 1°C accuracy and humidity range between 10% - 99% RH using a probe which can test the air condition at any place.



Figure 33. Temperature humidity meter

Table 16: Specifications and performance of the temperature humidity meter

Variable	Description
Type:	Digital Thermometer Hygrometer
Temperature Range:	-50°C - 70°C
Measuring Humidity Range:	10% RH - 99% RH
Humidity Accuracy:	5%
Temperature Accuracy:	1°C

3.2.8 Clamp ampere meter

GWM-039 in Figure 34 is an instrument measuring device utilized in this project to measure the current feed into compressor of the water dispenser in order to measure the electric consumed power. Features and specifications are stipulated in Table 17.



Figure 34. Clamp ampere meter

Table 17. Specifications and performance of the clamp ampere meter

Display	3 1/2 digits LCD display
Power source	AAA x 4pcs
Accessories	Instruction manual x 1 , Test lead x 1 Alligator x 1, Carrying case x 1
Dimension & weight	85(W)x43(H)x270(D) mm Approx. 700g
AC current	
Range	35A, 350A, 1000A 3ranges
Accuracy	47Hz~63Hz (1% rdg+5digits)

3.3 Safety Rules

In order to achieve the objectives of this project, safety rules were set inside the laboratory and they are listed below:

- 1) Ensure the availability of fire extinguisher.
- 2) Ensure that the engine's exhaust pipe are set outside the lab properly prior starting the engine.
- 3) Ensure evacuating fan is on all the time during the experiment.
- 4) Probe tip of gas analyzer and the smoke meter has to be always clean.
- 5) The sampling test probe has to be fully inserted into the exhaust pipe when testing exhaust emission.
- 6) Ensure wearing all personal protective equipment (PPE) while commencing the works (i.e. dust mask, gloves, goggles, etc...)

CHAPTER 4: RESULTS AND DISCUSSIONS

This chapter refers to the data that have been acquired during the experiments and depicted into graphs. These graphs are analyzed to show the impact of different tested inlet air temperatures at a constant absolute humidity for two cases; constant load and constant speed. Section 4.1 discusses the effect of varying inlet air temperatures on the performance of the engine, while in section 4.2 the discussion is about the effect of varying inlet air temperatures on emissions and smoke.

4.1 Effect of varying inlet temperature on engine performance

This section compares and studies the effect of inducing 3 different inlet air temperatures into the engine in terms of combustion and performance characteristics.

4.1.1 Combustion Characteristics

- Pressure-Crank Angle Diagram

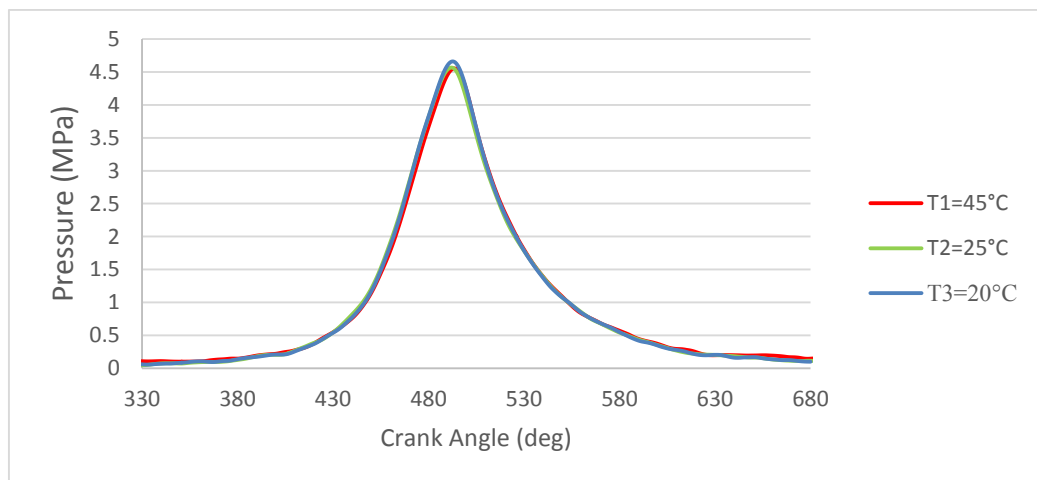


Figure 35. Cylinder pressure vs. crank angle for three different inlet temperatures

Figure 35 shows how cylinder pressure changes over crank angle for three different inlet temperatures at speed = 2200 RPM and a load 1.5 N.m. Above plot was exported for the range where the upcoming characteristics are focused on, it shows the range of crank rotation at the beginning of compression stroke where it begins at start of injection (SOI) before top dead center (approximately 20° bTDC) followed by start of combustion (SOC) and then peaks towards top dead center (TDC) through where TDC highest level in the cylinder during compression stroke (around 360°). The period between SOI and SOC is the ignition delay (ID)

Figure 35 depicts the pressure rise while running at three induced air temperatures. It is observed that the pressure rise for lower temperatures (at T1 and T2) are the highest. As inlet air temperature decreases, its density becomes higher and results in better fuel-injection atomization and more complete combustion, which consequently increases the peak pressures after having relatively longer ignition delay. [15]

Prior showing the results, Table 18 shows all uncertainties for the calculated parameters that will be presented in next sections.

Table 18. Uncertainty Table for calculated parameters

Speed of air	Air Mass flow rate	A/F ratio	Brake Power	BSFC	Volumetric Efficiency	Improved power	Electrical power	Gained Power
± 0.1 m/sec	± 0.0002 kg/sec	± 3	± 0.0001 kW	± 0.0006 kg/kWh	$\pm 0.002\%$	± 0.0001 kW	± 0.002 kW	± 0.003 kW

4.1.1.1 Constant Load

1) Maximum Cylinder Pressure

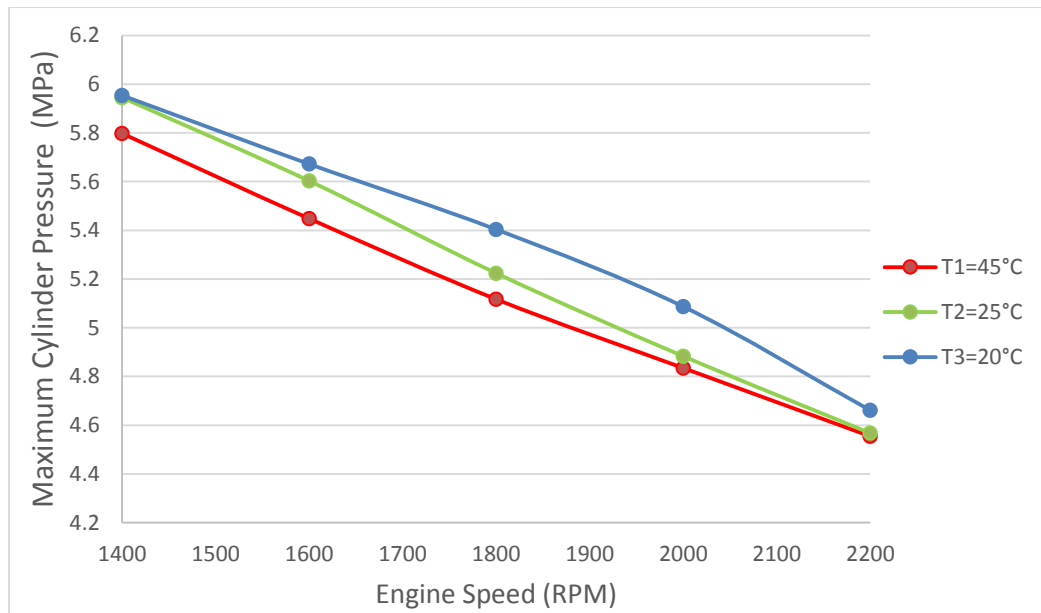


Figure 36: Maximum cylinder pressure vs. engine speed for three inlet temperatures

Figure 36 shows the changes of in-cylinder peak pressures with engine speed at three induced temperatures into the engine. It can be observed that as the engine speed

increases, engine peak pressure decreases. This is due to the fact that the mass flow rate of air increases when increasing engine speed and result better mixing which leads to a better combustion. Peak pressures were lowest at 45°C; however, peak pressures while running at 45°C converges to approximately 4.5 MPa similar to induced air at 25°C. On the other hand, cold induced air at 20°C had the highest peak pressure as the density of air is higher which slower mixer and retaining higher peak pressures at all different engine speeds [13].

2) Maximum pressure rise rate

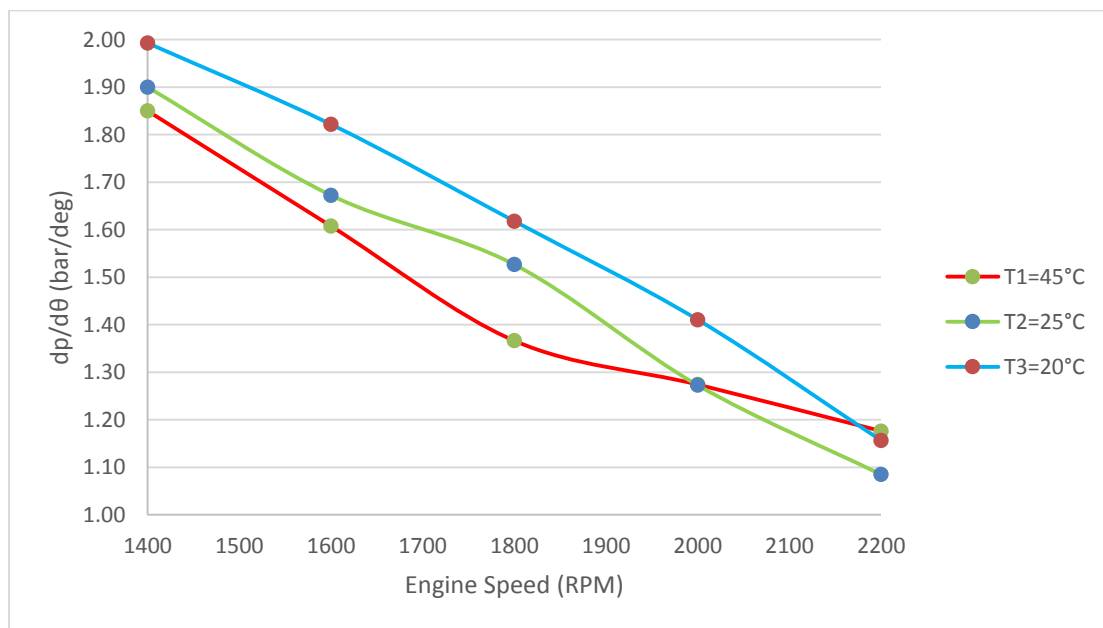


Figure 37. Maximum pressure riase rate vs. engine speed for three different inlet temperatures

Figure 37 indicates the relation between maximum pressure rise rates ($dp/d\theta$) with engine speed at three inlet temperatures. In compression ignition engine, atomization starts

between the injected fuel and compressed air then fires when fuel reaches its self-ignition temperature. The period of fuel atomization just before combustion in the engine cylinder is ignition delay (ID). If ID is longer, thus $dp/d\theta$ is larger as more fuel molecules concentrates with the compressed air. The faster the fuel particles burns, the smaller the peak pressure and eventually smaller $dp/d\theta$.

Figure 37 shows that the rate $dp/d\theta$ is higher while running at T1 and T2. This is due to peak pressures that were created due to longer ID that will consequently lead to better power output.

3) Heat release rate

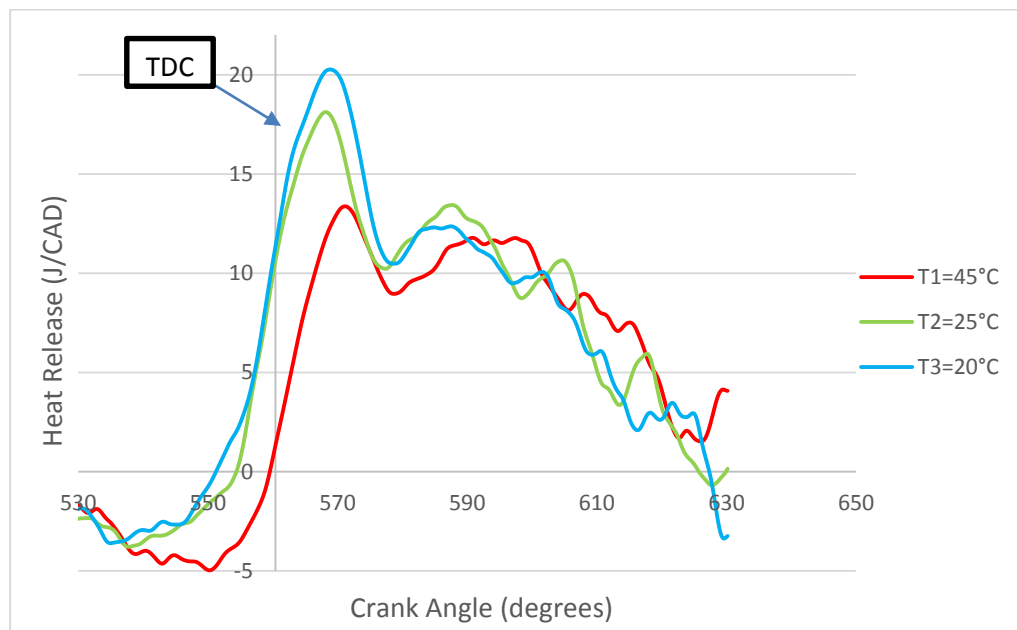


Figure 38: Heat release rate vs. crank angle at speed = 1800 RPM

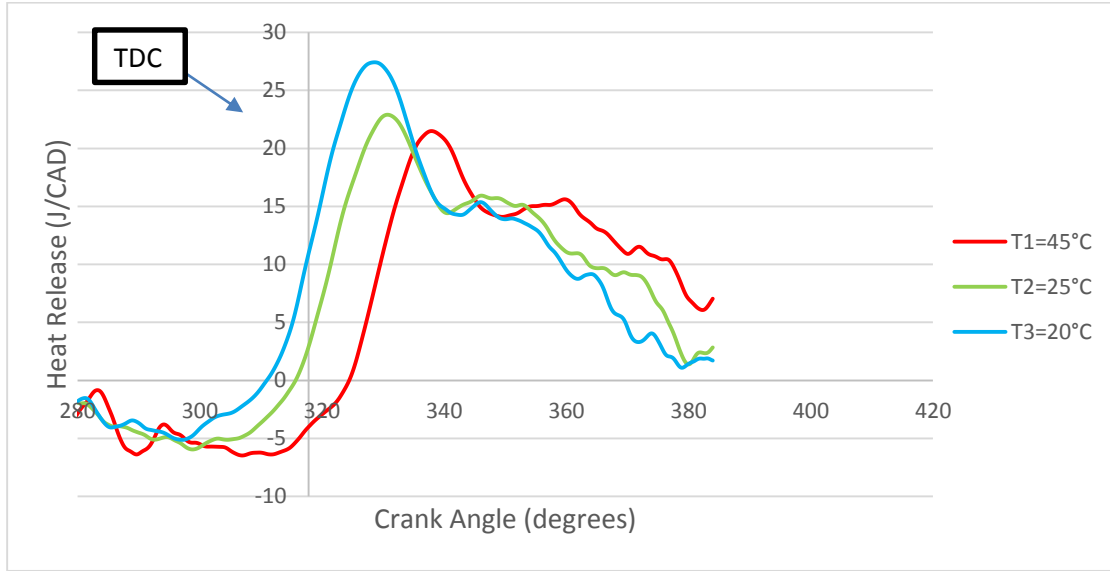


Figure 39: Heat release rate vs. crank angle at speed = 1600 RPM

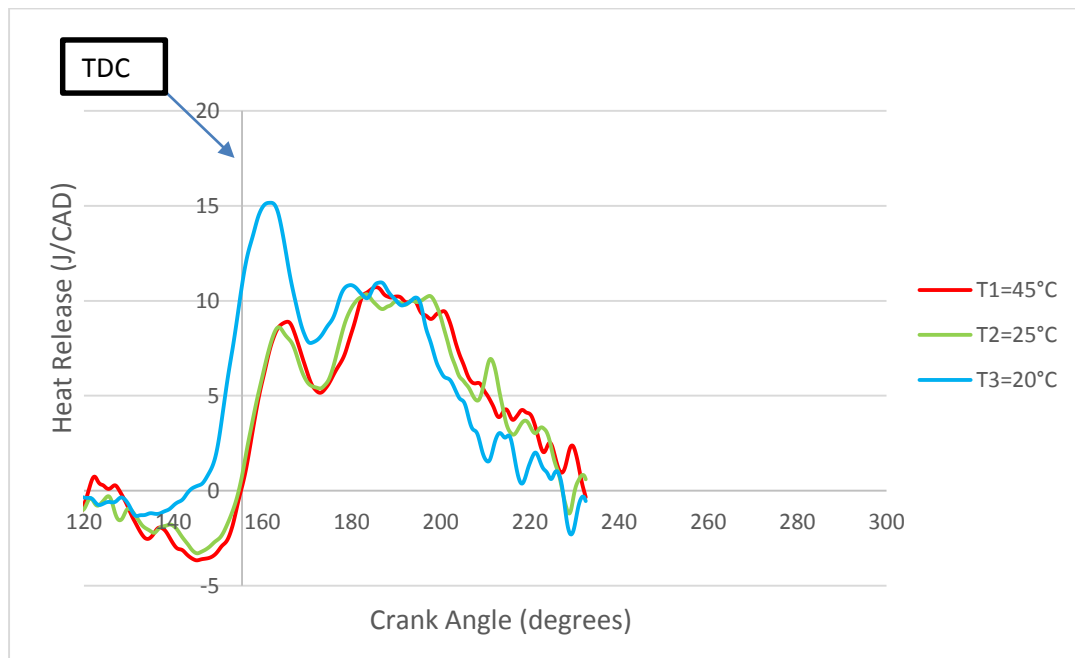


Figure 40: Heat release rate vs. crank angle at speed = 2000 RPM

Figures 38, 39 and 40 show the relation between in-cylinder heat release rates vs. crank angles at different engine speed running at three inlet temperatures. Heat release gives a direct indication how much power that can be achieved by an engine. The better A/F ratio will result in better atomization and efficient ignition delay; thus higher maximum in-cylinder pressure and finally maximum heat release during combustion [14].

As an instance in Figure 38, heat release rate is maximum while running at $T_2=20^\circ\text{C}$ as it has the highest A/F ratio then decreases when lowering inlet temperatures.

4.1.1.2 Constant Speed

1) Maximum cylinder pressure

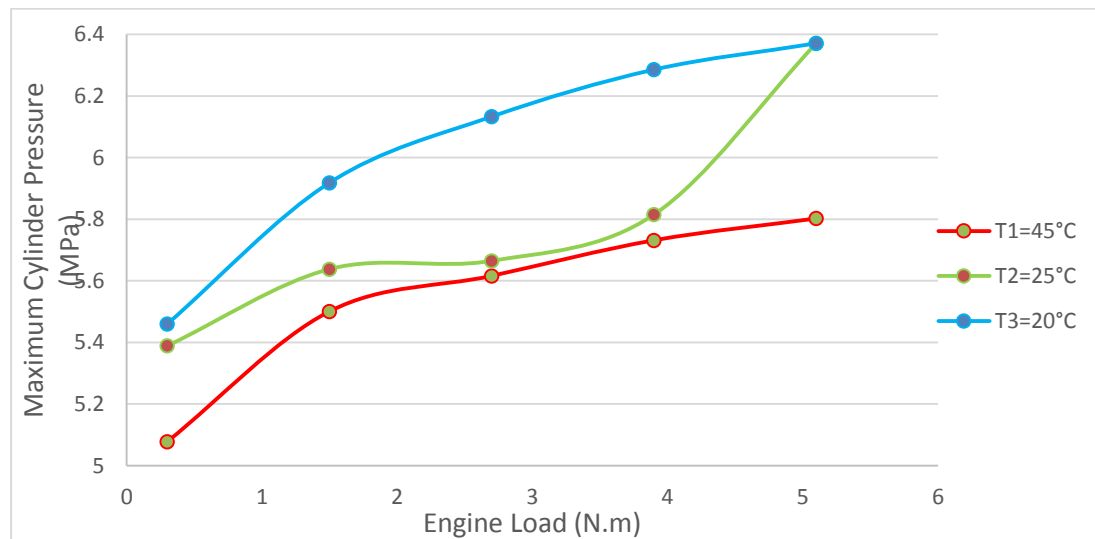


Figure 41: Maximum cylinder pressure vs. engine load for three inlet temperatures

Figure 41 represents changes of in-cylinder maximum pressure with load while running at three different induced temperatures into the engine. The peak pressure increases

with increasing the engine load due to the fact that the mass flow rate of air is kept constant when the engine speed is steady (=1600 rpm) while fuel injection is increasing, therefore the rate of mixing between air and fuel (atomization) is lower which delays the ignition period more. This results in higher in-cylinder peak pressures. [13]

It is worth mentioning that for lower temperatures the density of air induced into the engine is high which would result in relatively higher ID that would lead to higher cylinder peak pressures compared to hotter induced air as discussed in previous chapter.

2) Maximum pressure rise rate

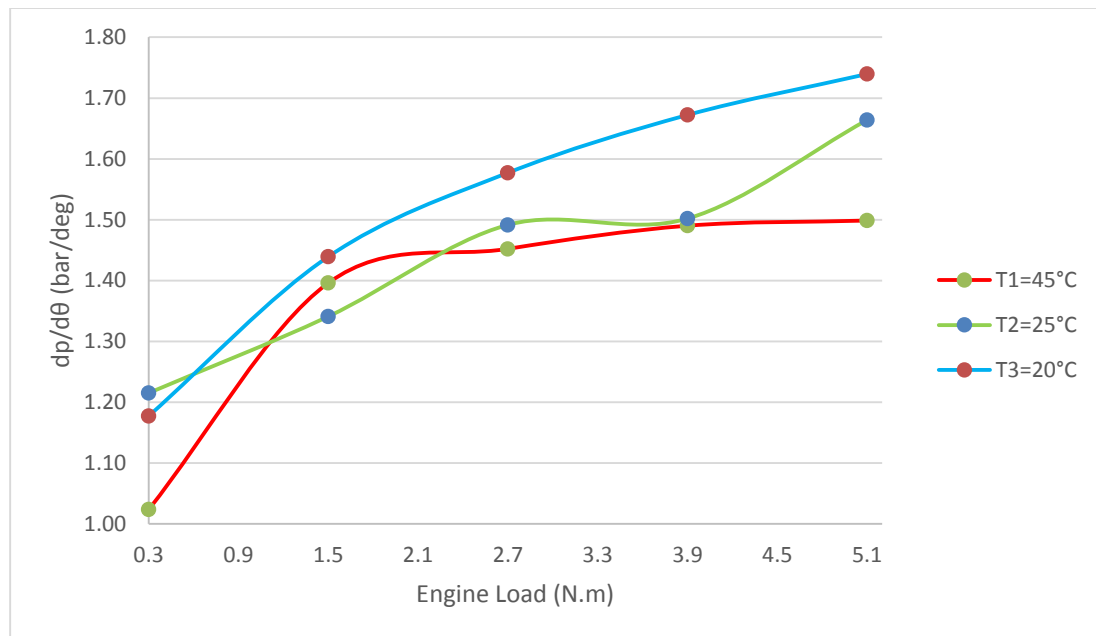


Figure 42: Maximum pressure rise rate vs. engine load for three different inlet temperatures.

Figure 42 describes the rate of change of pressure with crank angle with engine load while running at three different induced temperatures. As discussed earlier, the higher $dp/d\theta$, the longer the ignition delay period which will result in lower engine combustion rates if exceeded limits. As noticed from Figure 42 shows a higher rate of change of pressure with crank angle when running at T1 and T2 due to longer ignition delay which results in having leaner A/F mixtures that improved overall engine power output.

3) Heat release rate

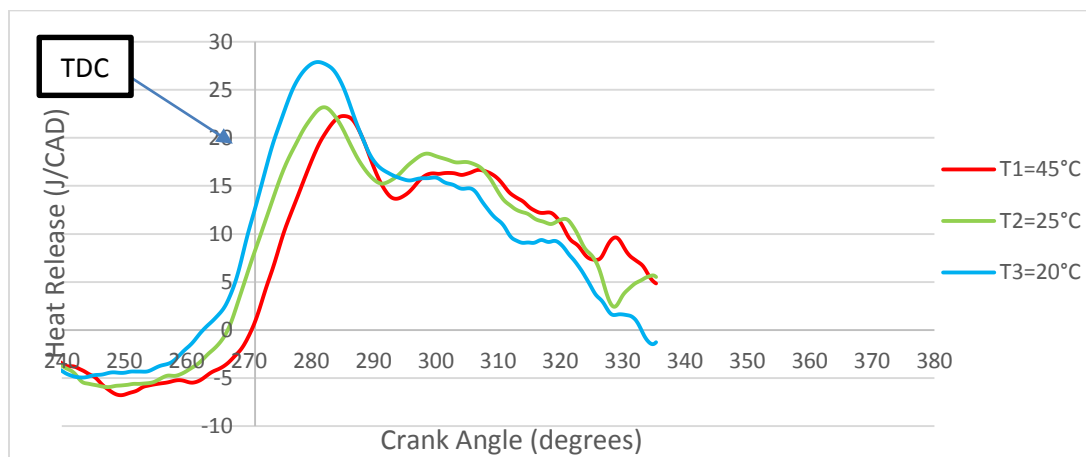


Figure 43: Heat release vs. crank angle at load = 1.5 N.m for three different inlet temperatures

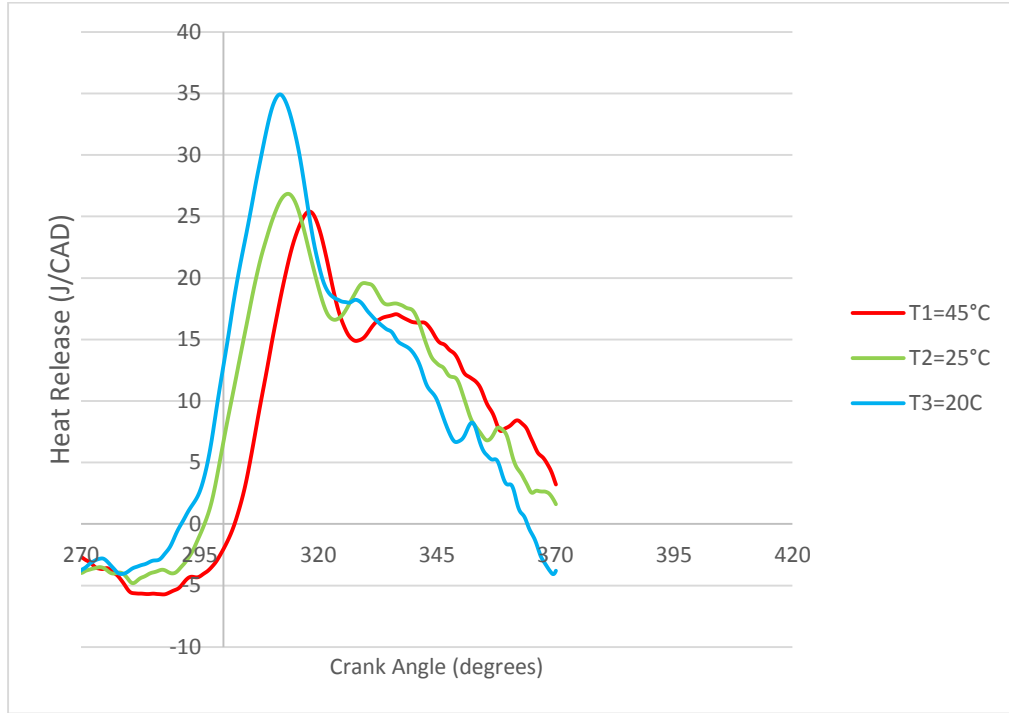


Figure 44: Heat release vs. crank angle at engine load = 3.9 N.m for three different inlet temperatures

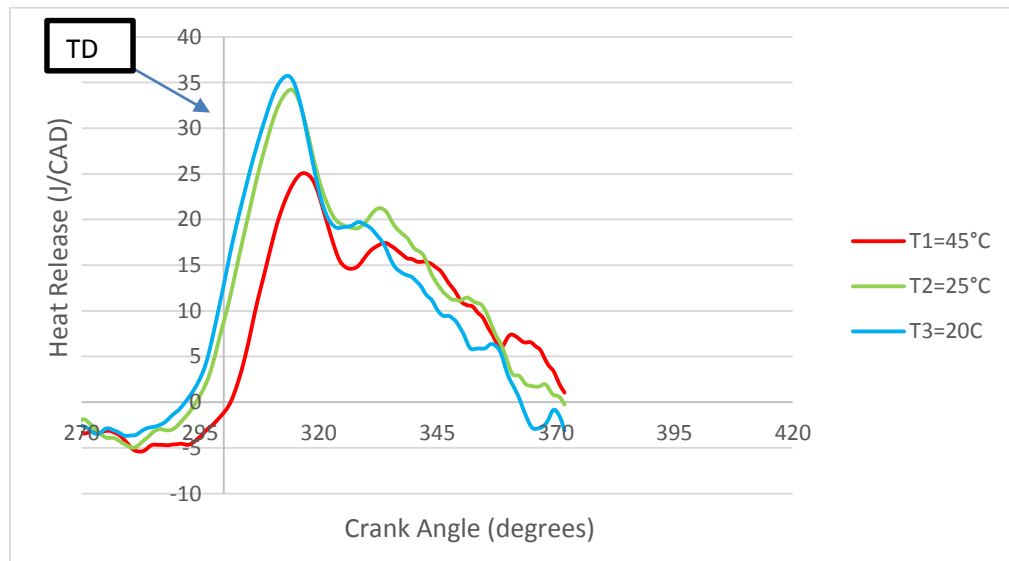


Figure 45. Heat release vs. crank angle at engine load = 5.1 N.m for three different inlet temperatures

Figures 43, 44 and 45 depicts the relation between heat release rates with crank angle at different engine loads while running at different inlet temperatures. The calculation of heat release rate including the equation used and calculations can be found in Appendix B for reference. It can be seen that heat release is maximum for T1 and T2 comparing when running at T3. Hence, running at lower temperatures increases A/F ratio [15] and enhances mixing with injected fuel at higher loads. As a result, higher peak pressures that leads for more heat release and eventually more power output.

4.1.2 Performance Characteristics.

4.1.2.1 Constant Load

1) Air-to-Fuel Ratio

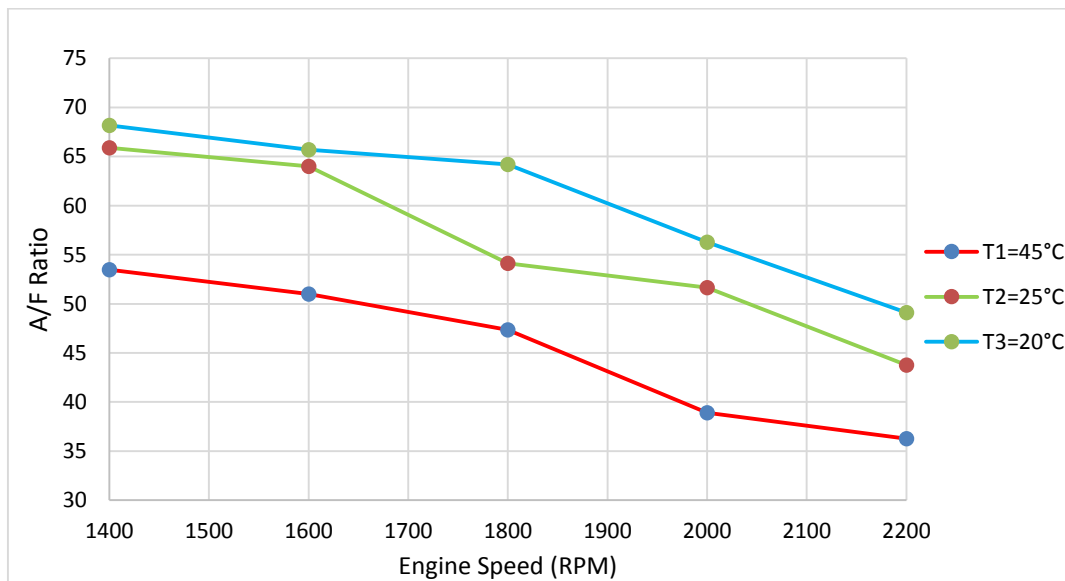


Figure 46: Air-to-fuel ratio vs. engine speed for three inlet temperature

Figure 46 shows the effect of different inlet temperatures on A/F ratio governed by the engine. It can be observed that A/F decreases with increasing engine speed and this is due to the fact that more air mass flow rate is being drawn into the engine which will result in having more fuel being injected to complete the combustion [15]. However, as induced temperature decreases, its mass increases which will result in a higher air to fuel ratio as represented by equation 4. It is worth mentioning from the literature that A/F ratio for naturally aspirated diesel engine ranges between 18 to 70 [3]. A/F ratio has increased by 27.5% for T2 at 20°C compared to T3 at 45°C.

$$\frac{A}{F} = \frac{\dot{m}a}{\dot{m}f} \quad \dots\dots \text{Equation (4)}$$

2) Volumetric Efficiency

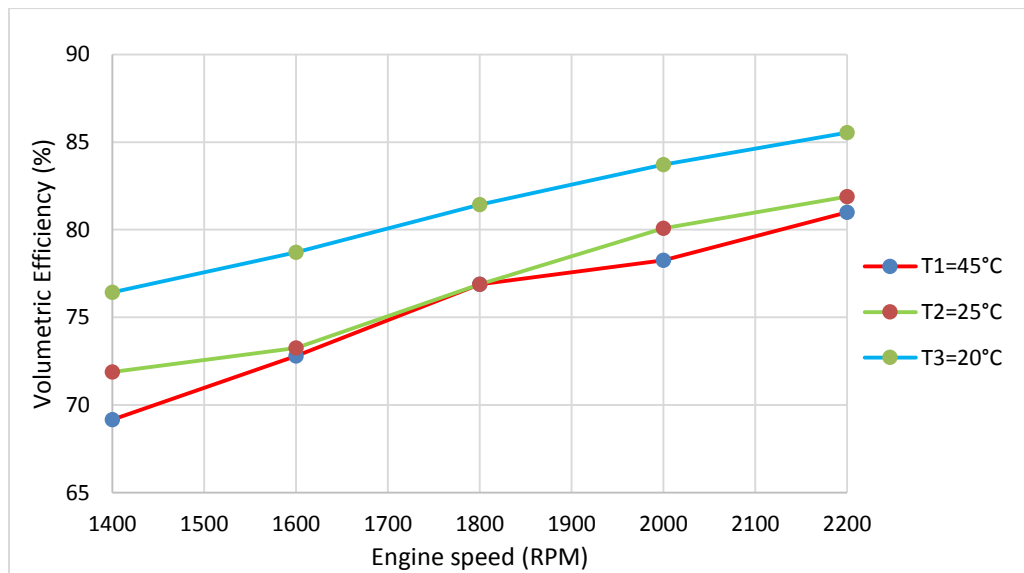


Figure 47: Volumetric efficiency vs. engine speed for different inlet temperatures

Volumetric efficiency is a measure of how effective the engine's induction system and the biggest constraints that lead to lower efficiency are; frictional flow and choked flow hence this also includes intake system components (i.e. air filter, inlet manifold, etc...). Figure 47 explicitly shows the superior volumetric efficiency at T2 governed by its high air density at cold 20°C and this is can be concluded from Equation 5.

$$\eta_v = \frac{2\dot{m}a}{\rho_a V d N i} \dots\dots \text{Equation (5)}$$

η_v : Volumetric Efficiency

N: Engine Speed (RPM)

\dot{m} : Air mass flow rate

V_d : Cylinder volume

ρ_a : Density of air at inlet manifold

i: Number of engine cylinders

3) Brake Specific Fuel Consumption

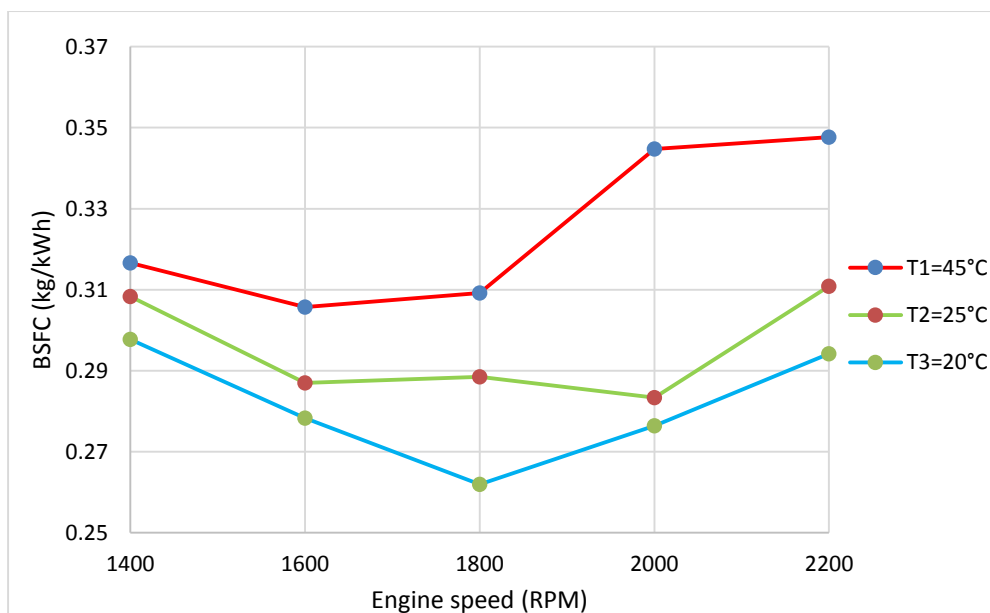


Figure 48: Brake specific fuel consumption vs. engine speed at different inlet temperatures

Figure 48 illustrates the relation between brake specific fuel consumption (BSFC) with engine speed at three different inlet temperatures. BSFC gives an indication that the quality of the air-to-fuel mixing and who economical fuel consumption is with reference to Equation 6. It can be observed from Figure 48 that T2 gives the minimum BSFC which is also proved by having the highest volumetric efficiency compared to other inlet temperatures [16].

$$BSFC = \frac{\dot{m}_f}{P_b} \dots \text{Equation (6)}$$

BSFC: Brake Specific Fuel Consumption

\dot{m}_f : Fuel mass flow rate

P_b: Brake Power

4) Gained Power

In order to analyze the increase in the engine power due to reducing the air temperature using the developed cooling system, it is required to check the total gained power by the engine. Accordingly, fuel mass flow rate for T3 which is the reference temperature in summer was set constant to calculate the improved power for T1 and T2 using Equation 6 with reference to Tables 19 and 20. After that the gained power was calculated using Equation 7.

$$PG = PI - PE \dots \text{Equation (7)}$$

PG: Gained Power

PI: Improved Power

PE: Electrical Power consumed via the compressor of the cooling system

Table 19. Gained power for T1 = 25°C at constant load.

Load (N.m)	Fuel Mass Flow (kg/h)	BSFC (kg/kWh)	Improved Power (kW)	Power Consumed from Cooling System (kW)	Gained Power (kW)
1400	0.28	0.28	0.98	0.15	0.826
1600	0.31	0.26	1.18	0.15	1.023
1800	0.35	0.29	1.21	0.15	1.060
2000	0.43	0.28	1.53	0.15	1.376
2200	0.48	0.31	1.55	0.15	1.394

Table 20: Gained power for T2 = 20°C at constant load

Load (N.m)	Fuel Mass Flow (kg/h)	BSFC (kg/kWh)	Improved Power (kW)	Power Consumed from Cooling System (kW)	Gained Power (kW)
1400	0.28	0.30	0.93	0.15	0.783
1600	0.31	0.28	1.10	0.15	0.952
1800	0.35	0.26	1.33	0.15	1.183
2000	0.43	0.28	1.57	0.15	1.415
2200	0.48	0.29	1.63	0.15	1.481

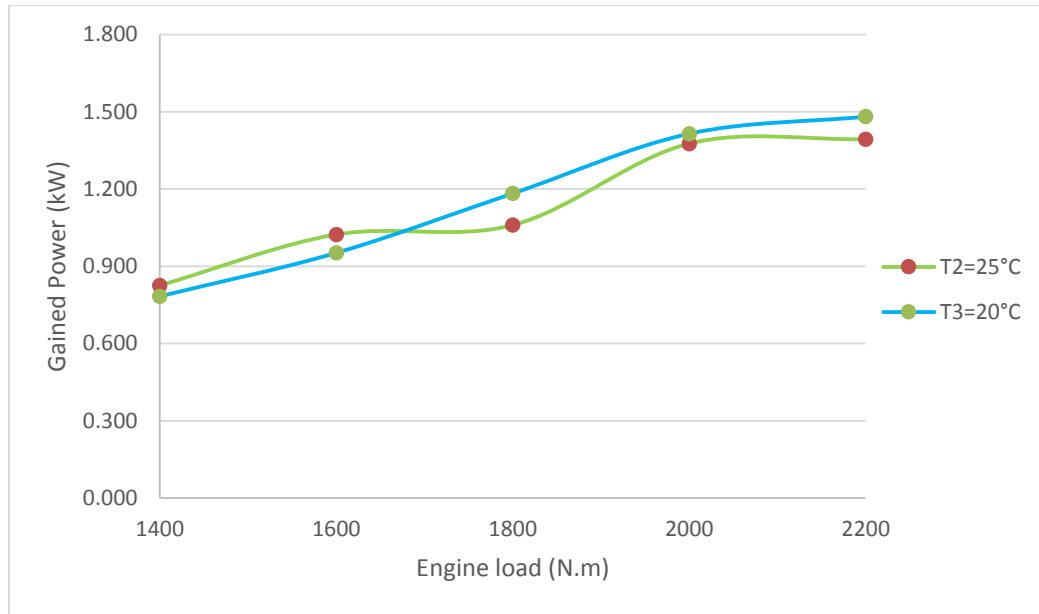


Figure 49: Gained power vs. engine speed while running at T1 and T2

Figure 49 shows the relationship between gained power and engine speed while running at T1 and T2. It can be detected that as the speed increases, the gained power by the engine is increasing as well. Running at T1 and T2 at lower speed does not give much benefits in terms of power however at higher speed it can be seen that running with T2 increases the gained power by 6% comparing to T1.

5) Gained Energy

Another parameter that is essential to calculate the energy gained by the engine keeping into consideration the electrical energy consumed by the cooling system. Similarly, fuel mass flow rate for T3 was set constant to calculate gained energy while running at T1 and T2. Tables 21 and 22 stipulate all calculated data. Gained energy was

calculated using Equation 8.

$$GE = GP \times \text{Time} \dots \text{Equation (8)}$$

GE: Gained Energy

GP: Gained Power

Time: Time taken in hours to cool down the air temperature to the required set point

Table 21. Gained energy for T1 = 25°C at constant load

Improved Power (kW)	Time (hours)	Electric power (KW)	Electrical Energy Consumed (kWh)	Improved Energy (kWh)	Gained Energy (kWh)
0.98	0.12	0.15	0.018	0.12	0.099
1.18	0.12	0.15	0.018	0.14	0.122
1.21	0.12	0.15	0.018	0.14	0.127
1.53	0.12	0.15	0.018	0.18	0.164
1.55	0.12	0.15	0.018	0.18	0.167

Table 22: Gained energy for T2 = 20°C at constant load

Improved Power (kW)	Time (hours)	Electric power (KW)	Electrical Energy Consumed (kWh)	Improved Energy (kWh)	Gained Energy (kWh)
0.93	0.2	0.15	0.030	0.19	0.157
1.10	0.2	0.15	0.030	0.22	0.190
1.33	0.2	0.15	0.030	0.27	0.237
1.57	0.2	0.15	0.030	0.31	0.283
1.63	0.2	0.15	0.030	0.29	0.26

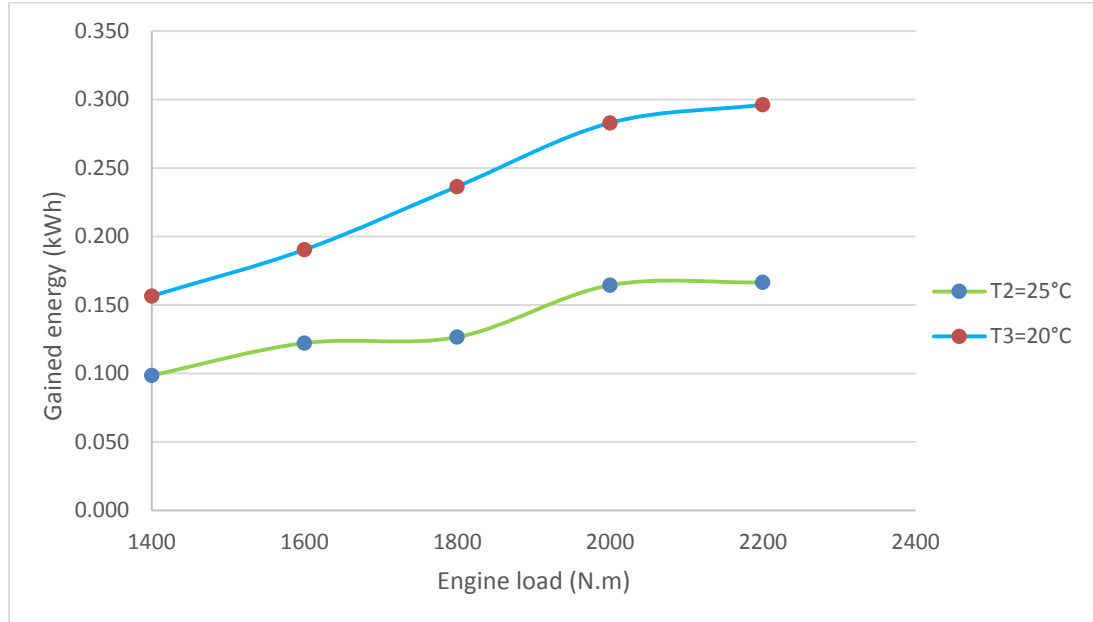


Figure 50: Gained energy vs. engine speed while running at T1 and T2

Figure 50 represents the relationship between gained energy and engine speed while running at T1 and T2. It can be observed that as the speed increases, the energy gained by the engine is increasing as well. However, at T2 the gained energy is way higher at all speeds and reaches up to 78% higher than T1.

4.1.2.2 Constant Speed

1) Air-to-Fuel Ratio

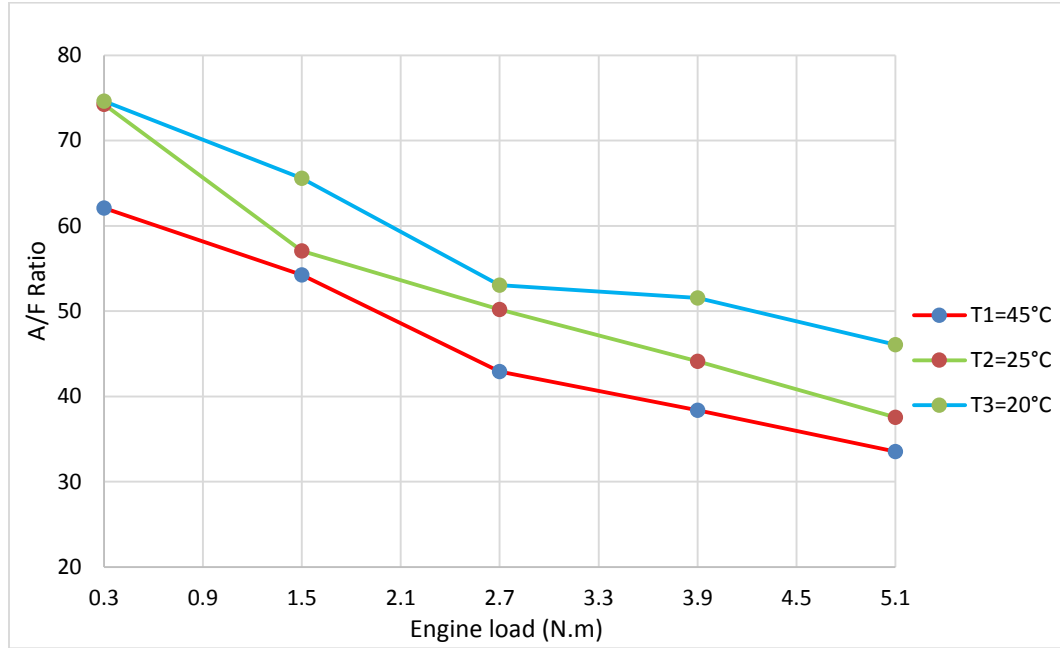


Figure 51: Air-to-Fuel ratio vs. engine load for three different inlet temperatures

Figure 51 describes the relation between A/F ratio and engine load at three different induced temperatures. It is observed that as the engine load increases, A/F ratio decreases and this is due to the fact the air mass flow rate is steady with the addition of more fuel to complete the combustion. Running at T2 still gives a better A/F than running with T1 and T3.

2) Volumetric Efficiency

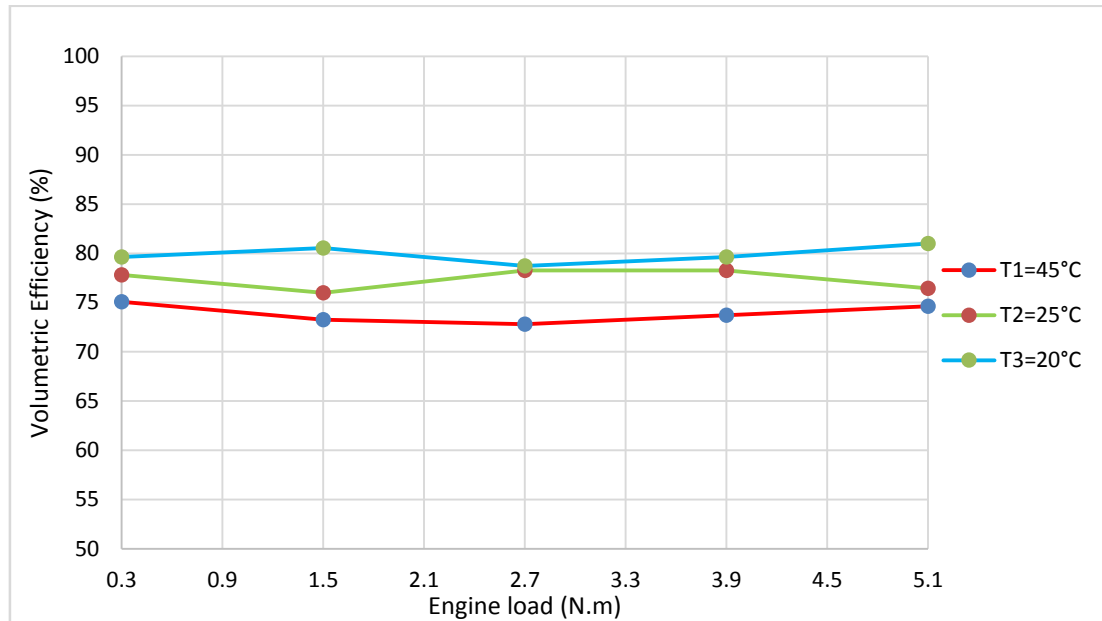


Figure 52: Volumetric efficiency vs. engine load at three different inlet temperatures

Figure 52 shows the relationship between volumetric efficiency and Engine load for three different temperatures. It shows a noticeable increase in volumetric efficiency while running the engine at T2.

3) Brake Specific Fuel Consumption

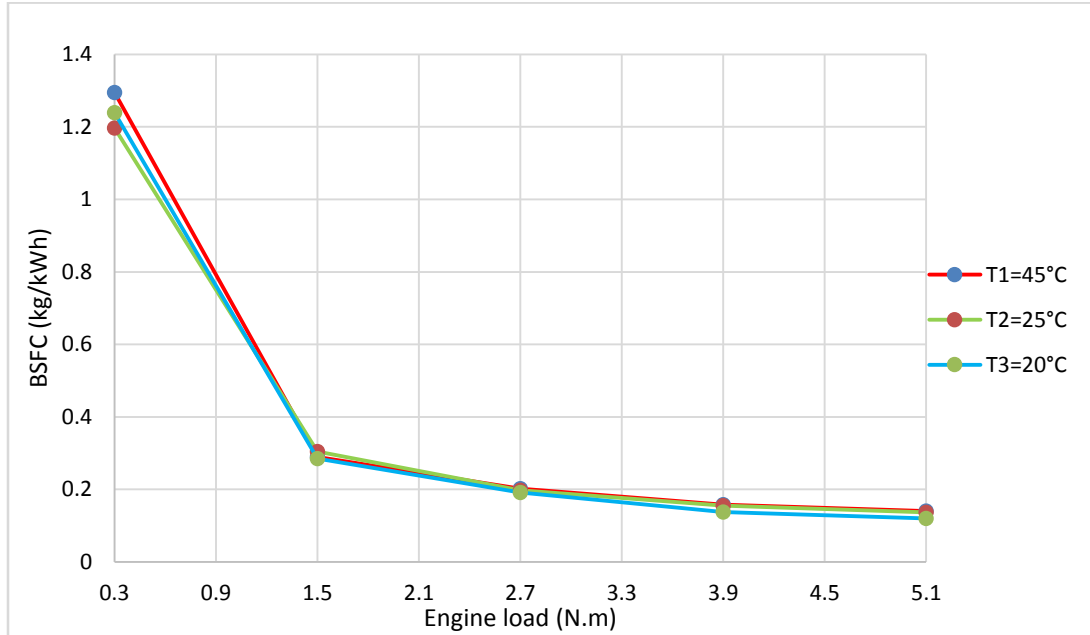


Figure 53: BSFC vs. engine load for three different inlet temperatures

Figure 53 depicts the relationship between BSFC and engine load at three different inlet air temperatures. It can be noticed that running at T2 has relatively lower BSFC compared when running at T1 and T3 for higher loads and that also confirms with chapter 4.1.2.1.

4) Gained Power

Similar to what have been discussed in section 4.1.2.1, fuel mass flow rate for T3 was set constant to calculate the improved power for T1 and T2 with reference to Tables 23 and 24.

Table 23: Gained power for T1 = 25°C at constant speed

Load (N.m)	Fuel Mass Flow (kg/h)	BSFC (kg/kWh)	Improved Power (kW)	Power Consumed from Cooling System (kW)	Gained Power (kW)
0.3	0.26	1.20	0.22	0.15	0.07
1.5	0.29	0.30	0.96	0.15	0.80
2.7	0.37	0.20	1.84	0.15	1.69
3.9	0.41	0.16	2.65	0.15	2.50
5.1	0.48	0.14	3.50	0.15	3.35

Table 24: Gained power for T2 = 20°C at constant speed

Load (N.m)	Fuel Mass Flow (kg/h)	BSFC (kg/kWh)	Improved Power (kW)	Power Consumed from Cooling System (kW)	Gained Power (kW)
0.3	0.26	1.24	0.21	0.15	0.06
1.5	0.29	0.29	1.02	0.15	0.87
2.7	0.37	0.19	1.91	0.15	1.75
3.9	0.41	0.14	3.00	0.15	2.85
5.1	0.48	0.12	3.99	0.15	3.84

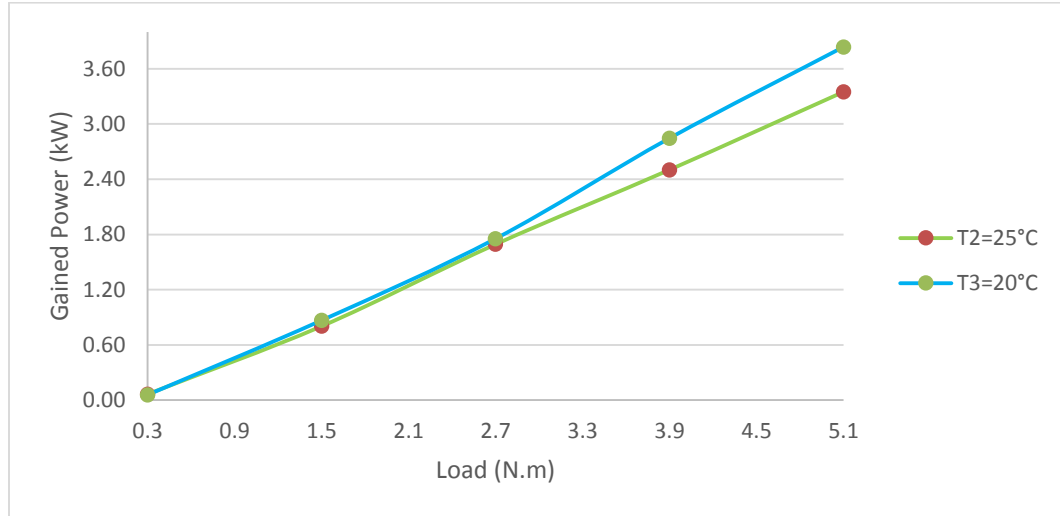


Figure 54: Gained power vs. engine load while running at T1 and T2

Figure 54 represents the relationship between gained power and engine load while running at T1 and T2. It is clear that the gained power increases as the engine load increases. It is worth mentioning that having lower temperatures at lower loads does not outweigh the necessity of the cooling system. However, at approximately 3 N.m engine load, T2 shoots up to 14% comparing to T1.

5) Gained Energy

Keeping the same fuel mass flow rate for T3 to calculate gained energy for T1 and T2 with reference to Tables 25 and 26.

Table 25: Gained energy for T1 = 25°C at constant speed

Improved Power (kW)	Time (hours)	Electric power (KW)	Electrical Energy Consumed (kWh)	Improved Energy (kWh)	Gained Energy (kWh)
0.22	0.12	0.15	0.018	0.025979196	0.008
0.96	0.12	0.15	0.018	0.114142658	0.096
1.84	0.12	0.15	0.018	0.220434883	0.202
2.65	0.12	0.15	0.018	0.317159923	0.299
3.50	0.12	0.15	0.018	0.41828404	0.400

Table 26: Gained energy for T2 = 20°C at constant speed

Improved Power (kW)	Time (hours)	Electric power (KW)	Electrical Energy Consumed (kWh)	Improved Energy (kWh)	Gained Energy (kWh)
0.21	0.2	0.15	0.030	0.042003659	0.012
1.02	0.2	0.15	0.030	0.20376932	0.173
1.91	0.2	0.15	0.030	0.381212178	0.351
3.00	0.2	0.15	0.030	0.599415172	0.569
3.99	0.2	0.15	0.030	0.797666114	0.767

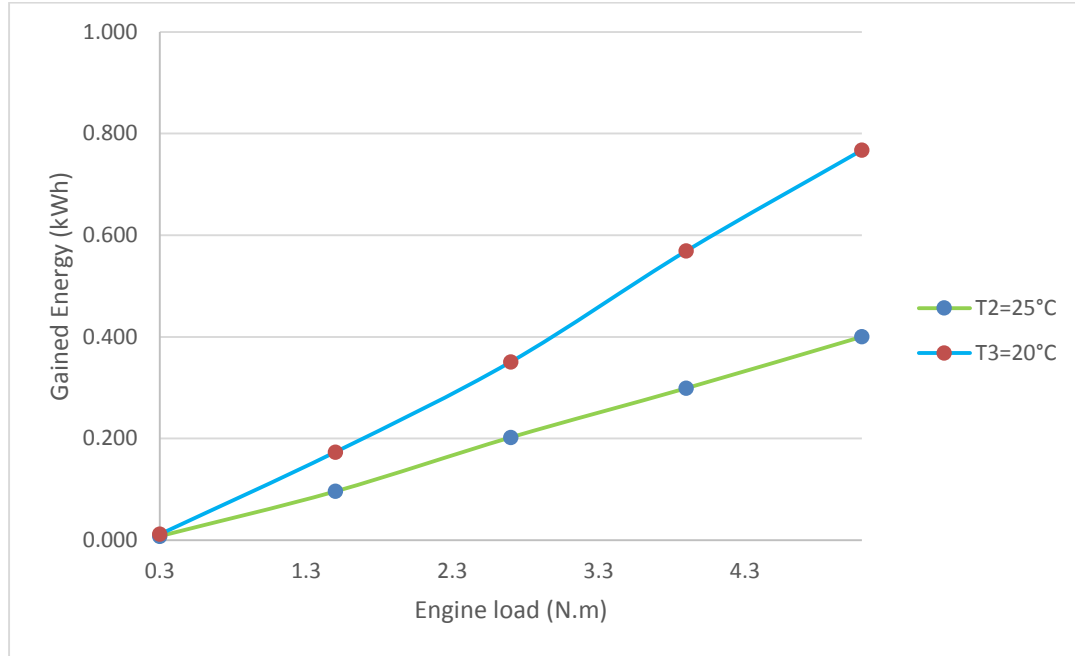


Figure 55: Gained energy vs. engine load while running at T1 and T2

Figure 55 represents the relationship between gained energy and engine load while running at T1 and T2. It can be seen that while running at T2, the gained energy of the engine shoots up to 92% comparing to T1.

4.2 Effect of varying inlet temperature on emissions and smoke

4.2.1 Constant Load

4.2.1.1) Emissions

4.2.1.1.1) NO_x

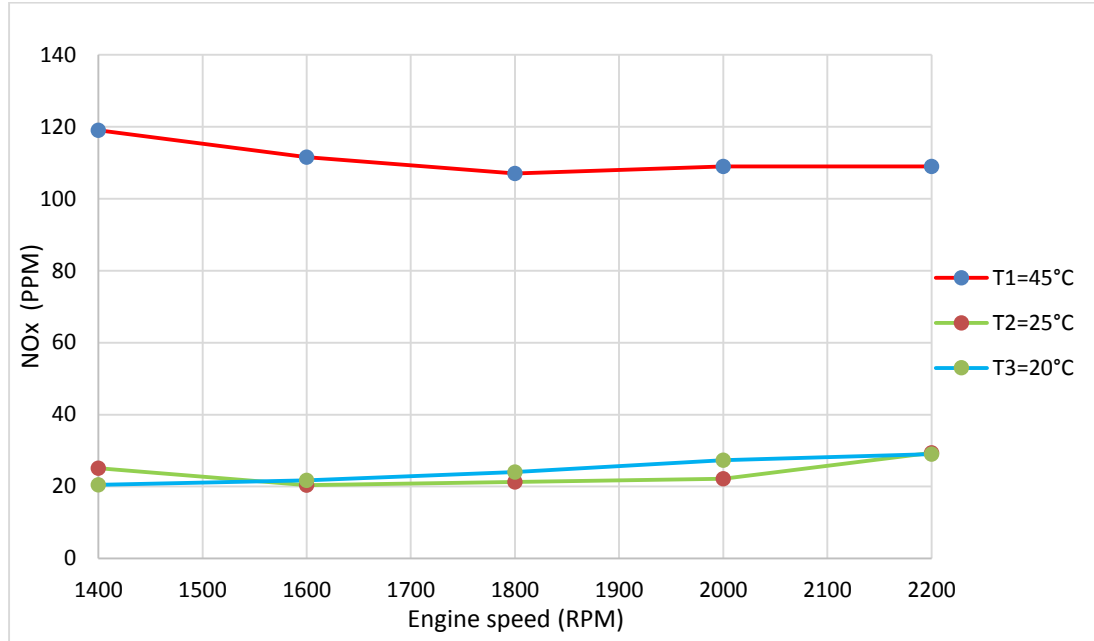


Figure 56: NOx vs. engine speed for three inlet temperatures

Nitric oxides (NOx) is a byproduct formed during combustion of engine oil due to reaction between nitrogen (N_2 – 70% of air) and oxygen (O_2) at elevated temperatures in excess of $1800^\circ C$. Figure 56 shows the relation between NOx and engine speed for three inlet different temperatures. As the engine speed increases, NOx emissions decreases as a result of decreased flame temperature. It is can be noticed from the graph above that as the inlet temperature decreases, over all in-cylinder peak temperatures reduces, accordingly NOx emissions decreases as well [17].

4.2.1.1.2) Hydrocarbon

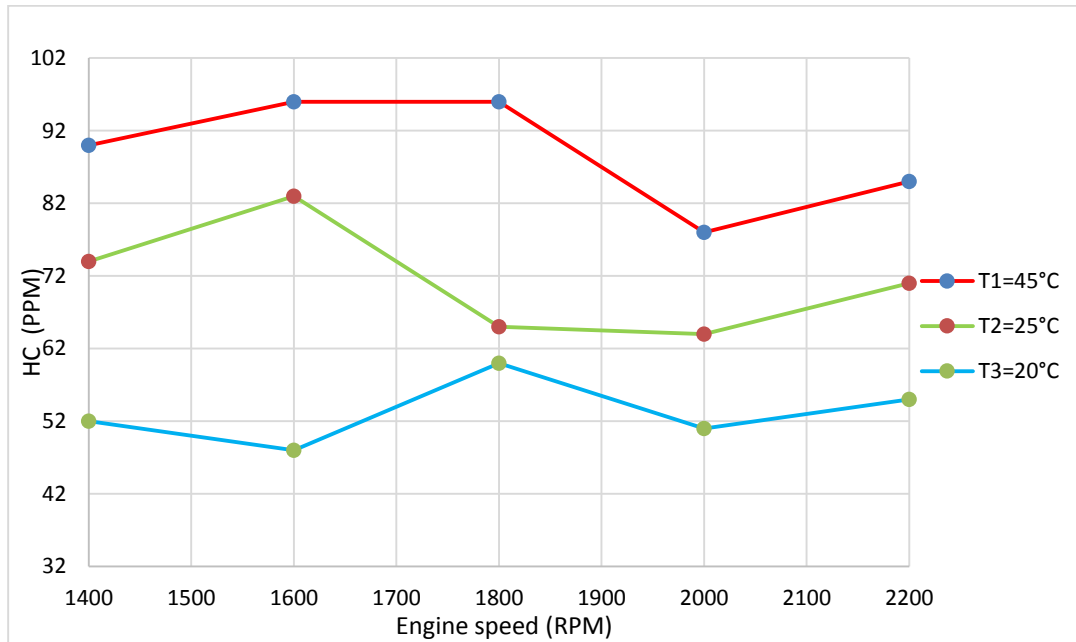


Figure 57: Hydrocarbon vs. engine speed for three different inlet temperatures

Figure 57 demonstrates the relationship between unburned hydrocarbons emissions against engine speed for three different inlet temperatures. Figure 57 shows a non-uniform change of HC emissions and not necessarily increasing nor decreasing. However, At T1 and T2 the level of released HC is considerably lower than T3. This due to the fact that A/F ratio at lower temperatures is high; as a result, will minimize injection of fuel to complete the combustion and consequently decreasing HC emissions [16].

4.2.1.1.3) CO₂

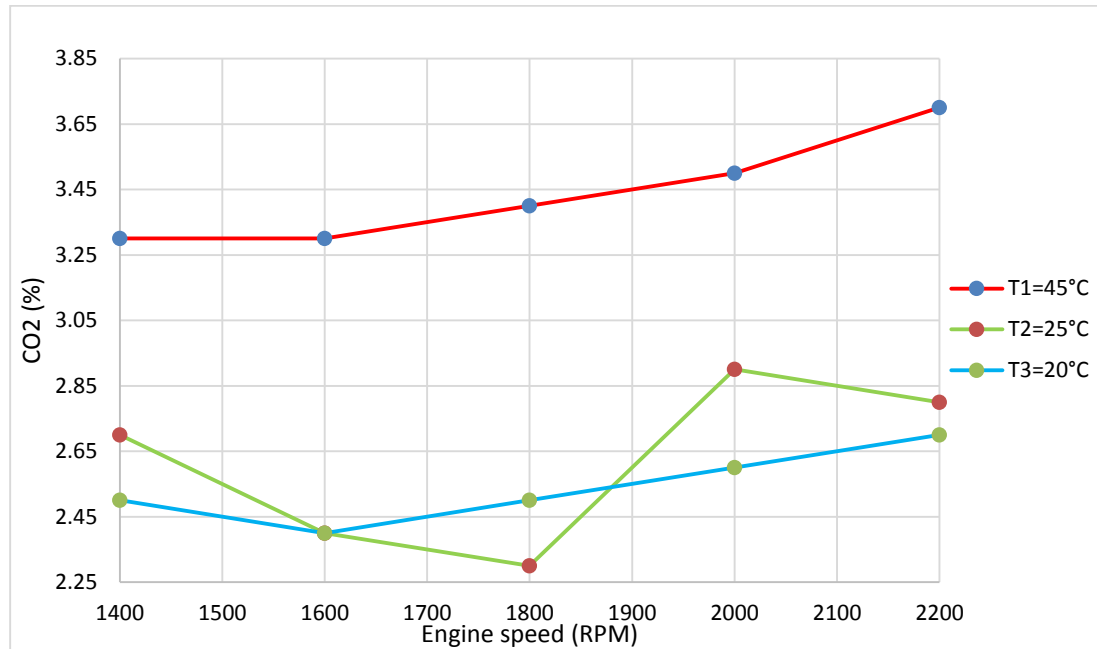


Figure 58: CO₂ vs. engine speed for three different inlet temperatures

Figure 58 describes the relationship between Carbon Dioxide emission rate and engine speed at three different inlet temperatures. CO₂ increases with increasing engine speed due to increasing air mass flow rate which oxidize the formed carbon monoxides inside the cylinder to form carbon dioxide. As noticed, reducing inlet temperatures results in reducing CO₂ emissions since mass of air is increased at lower temperatures which reduces the rate of carbon monoxides. Consequently, reducing oxidation rate to form carbon dioxide emissions [12].

4.2.1.2) Smoke emissions

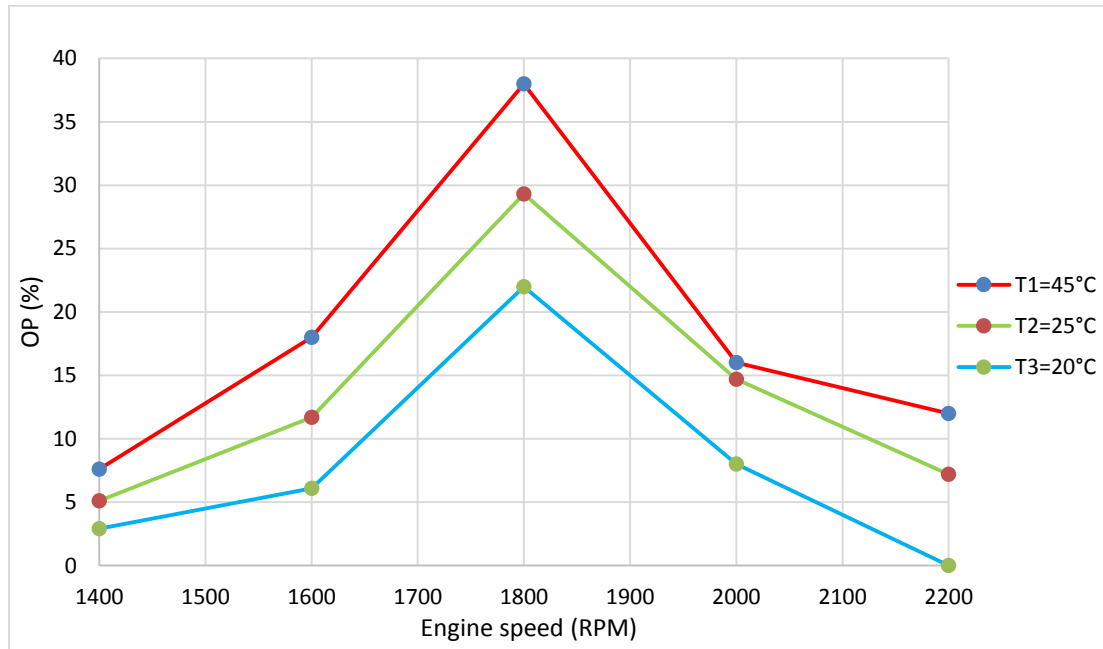


Figure 59: Smoke emission vs. engine speed for three different inlet temperatures

Figure 59 shows the relation between opacity and engine speed at three different inlet temperatures. It is observed that the change of smoke emissions is almost uniform for all inlet temperatures. Smoke emissions is increased with increasing exhaust temperatures and it is a result of particulates formed for incomplete combustion. Increasing the emissions especially at lower engine speed can be due to cold starting the engine and having incomplete combustion. However at higher speeds, the engine heats up and the rate of releasing smoke decreases with relative to decreasing HC emissions. Moreover, lower inlet air temperatures result in lower smoke emissions compared to others [13].

4.2.2 Constant Speed

4.2.2.1) Emissions

4.2.2.1.1) NO_x

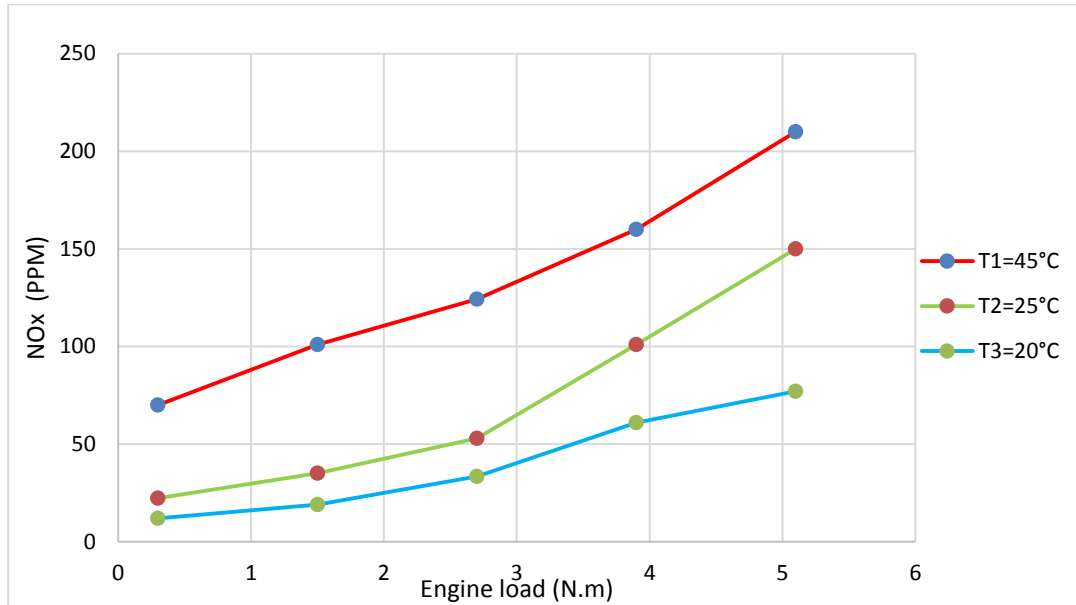


Figure 60: NO_x vs. engine load at three different inlet temperatures

Figure 60 shows the relationship between NO_x and Engine Load for three different inlet temperatures. It can be observed that NO_x emissions increase with increasing engine load and this is due to increasing overall temperatures inside the cylinder get higher which will result in higher NO_x emissions. On the other hand, as discussed in previous chapter, as inlet temperature decreases, the in-cylinder temperature decreases relatively and consequently reduces NO_x emissions. Reduction rate can reach up to 83% which is very considerably while running at T2.

4.2.2.1.2) Hydrocarbon

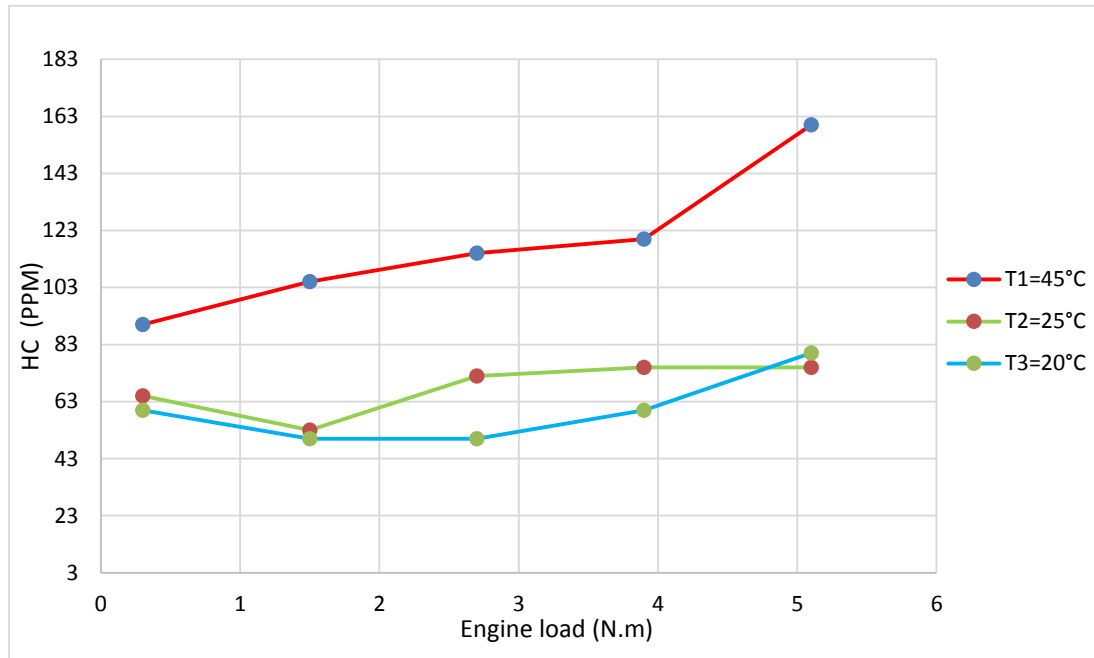


Figure 61: HC vs. engine load for three different inlet temperatures

Figure 61 shows the relationship between unburned hydrocarbon and engine load at three different induced temperatures. It can be noted that as the engine load increases more fuel will be injected into the cylinder at constant air mass flow rate to complete the combustion. As a result unburned HC emissions increase. Moreover, running at lower inlet temperatures has reduced the HC carbon due to inducing a denser mass of air into the cylinder which requires relatively less fuel to complete the combustion.

4.2.2.1.3) CO₂

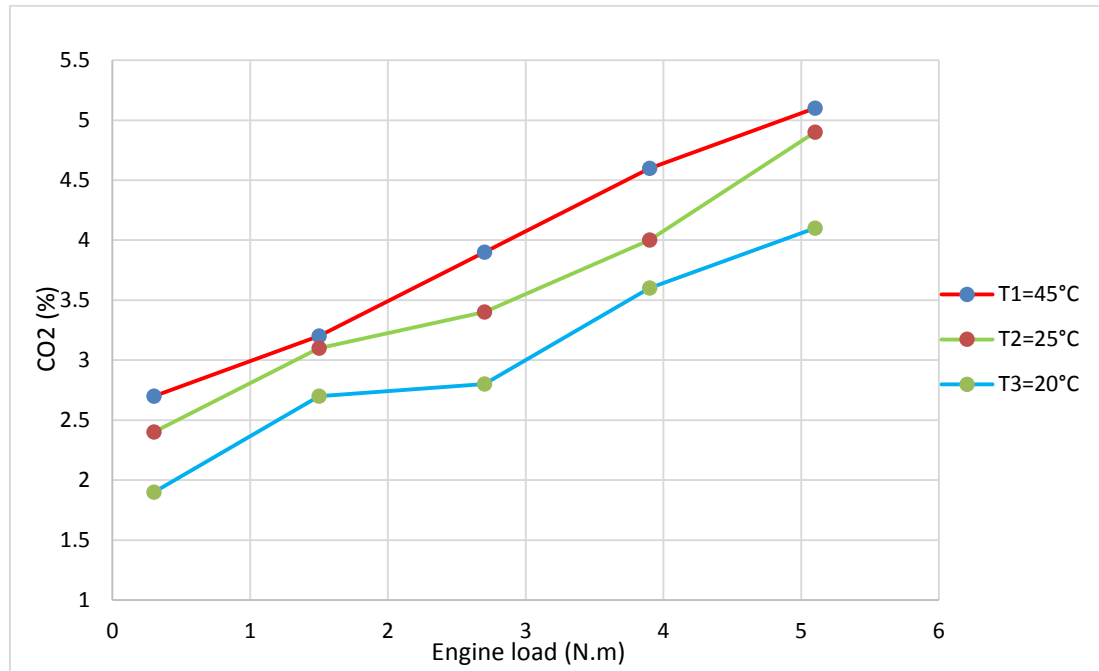


Figure 62: CO₂ emissions vs. engine load for three different inlet temperatures

Figure 62 describes the relation between carbon dioxide emissions and engine load for three different induced temperatures. It can be observed that nature of the graph remains the same while running at all temperatures, CO₂ emissions increases with increasing engine load. However, running at T2 has relatively lower emissions since the formation of carbon monoxide is less since the A/F is higher.

4.2.2.2) Smoke emissions

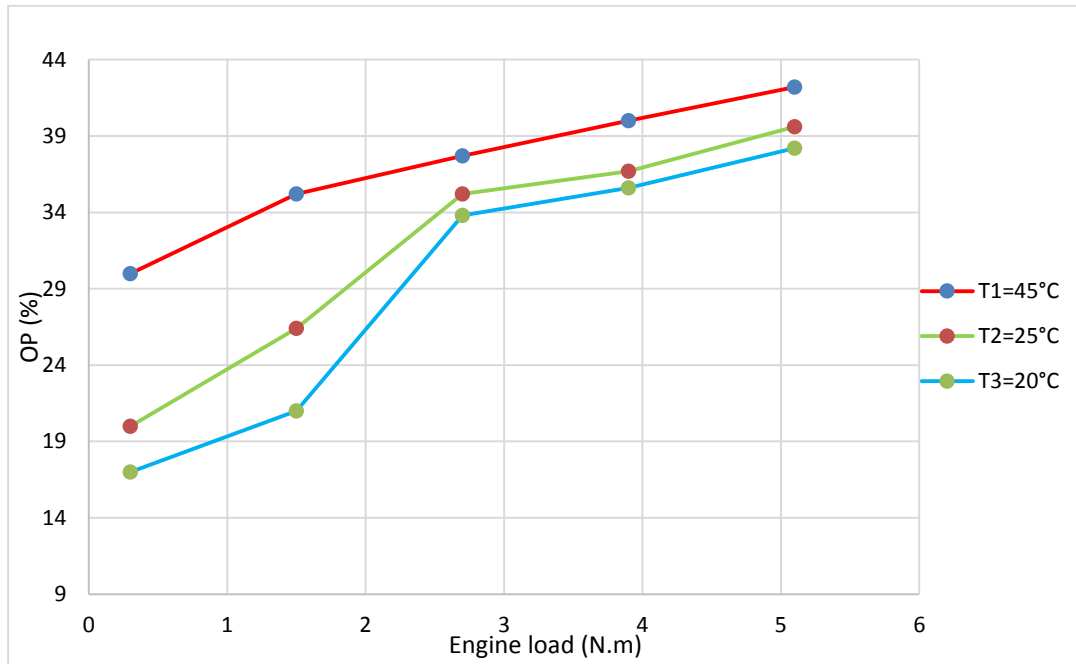


Figure 63: Opacity vs. engine load for three different inlet temperatures

Figure 63 shows the relation between smoke emissions (Opacity) and engine load for three different induced temperatures. Smoke production is directly linked to engine temperatures and incomplete combustion and forming large hydrocarbon fuel molecules which are cracked into carbon particles at high loads. Figure 63 shows the increasing nature of opacity with increasing engine load. However, running at lower inlet temperatures shall lower smoke emissions due to higher A/F than running in T3.

CHAPTER 5: CONCLUSION

In conclusion, this project studies the effect of inducing different inlet air temperatures on a naturally aspirated diesel engine running in July and located in QATAR. A test rig described in a single cylinder, four stroke, and naturally aspirated diesel engine was utilized to conduct all the experiments. The outcomes of the experiments covered engine's combustion, performance and emission characteristics.

The experiments have been conducted on a laboratory at Qatar University at approximately 22°C and 40% RH. Therefore, a temperature and humidity control design was developed to cope July's weather in QATAR as a reference case for this project (45°C and 45%). Followed by a cooling system that intends to cool the inlet air temperature to 20°C and 25°C via a thermostat at a constant absolute humidity.

After analysis, it was found that running the engine at 20°C inlet air temperature can maximize in-cylinder peak pressure by 60% at a constant load and increases volumetric efficiency of the engine by 11% (9% at a constant speed) at a constant load. Also, the smoke emission has decreased by 62% (43% at a constant engine speed) at a constant engine load. These improvements were due to increasing the air density which result in a better fuel-injection atomization and more complete combustion.

Finally, it was concluded that using a cooling system justifies its consumed power as the net gained power has increased by 7% (12% at a constant speed) at a constant load compared to the reference case. Therefore, utilizing an existing A/C of a vehicle and get it configured to the induction manifold can result in less cost modification of a vehicle, higher engine performance and a cleaner environment.

REFERENCES

1. CIMAC 2009, 'About the influence of ambient conditions on performance of gas engines', position paper at CIMAC conference, March 2009.
2. Climate and average monthly weather in Doha, Qatar. (2018). Retrieved from <https://weather-and-climate.com/average-monthly-Rainfall-Temperature-Sunshine,doha,Qatar>.
3. Heywood, J. B. (1988). Internal combustion engine fundamentals. New York: McGraw-Hill.
4. "Diesel Car" (Future Publishing Limited, July edition, 1993), p.104 Saber, H. a, Al-barwari, R. R. I., & Talabany, Z. J. (2013). Effect of Ambient Air
5. Woqod.com. (2019). Woqod. [online] Available at: <http://www.woqod.com/EN/Pages/default.aspx>
6. Kahandagamage, G. (2015). Analysis of the effect of charge air temperature and humidity on the combustion process of diesel engines at Heladhanavi Power Plant, Puttalam, Sri Lanka (Dissertation)
7. Kharseh, M., Al-Khawaja, M., & Suleiman, M. T. (2015). Potential of ground source heat pump systems in cooling-dominated environments: Residential buildings. *Geothermics*, 57, 104-110.
8. Mohd Muqem and Dr. Manoj Kumar, "Turbocharging of IC Engine: A Review", *International Journal of Mechanical Engineering and Technology (IJMET)*, Volume 4, Issue 1, 2012, pp. 142 - 149, ISSN Print: 0976 – 6340, ISSN Online: 0976 – 6359

9. Farrington, R. B., & Rugh, J. (2000). Impact of vehicle air-conditioning on fuel economy, tailpipe emissions, and electric vehicle range: preprint. Golden, CO: National Renewable Energy Laboratory.
10. Airconcars.com. (2019). AirconCars.com Car Air Conditioning Repair Aircon Manchester. [online] Available at: <http://www.airconcars.com/>
11. Turbosmart. (2019). Turbosmart - Blow off Valves, Wastegates, Boost Controllers, Fuel Pressure Regulators. [online] Available at: <https://www.turbosmart.com/>
12. Lin C. Y. and Jeng Y. L., (1996), Influences of charge air humidity and temperature on the performance and emission characteristics of diesel engines, Society of Naval Architects and Marine Engineers, Jersey City, NJ, ETATS-UNIS Volume 40, pp. 172-17.
13. Hsu, B.D. 2002, Practical diesel engine combustion analysis, Society of Automotive Engineers, Inc., USA.
14. Kadunic, S., Scherer, F., Baar, R., & Friedrich, I. (2014). Cool2Power - Increased petrol engine power and efficiency through an AC driven intercooling system. 11th International Conference on Turbochargers and Turbocharging, 3-12
15. Abdullah, N. R., Ismail, H., Michael, Z., Rahim, A. A., & Sharudin, H. (2015). Effects Of Air Intake Temperature On The Fuel Consumption And Exhaust Emissions Of Natural Aspirated Gasoline Engine. *Jurnal Teknologi*, 76(9). doi: 10.11113/jt.v76.5639

16. Chang, Y., Mendrea, B., Sterniak, J., & Bohac, S. V. (2015). Effect of Ambient Temperature and Humidity on Combustion and Emissions of a Spark Assisted Compression Ignition Engine. *Volume 1: Large Bore Engines; Fuels; Advanced Combustion*. doi: 10.1115/icef2015-1152
17. R.Margary, E.Nino,C. Vafidis. The effect of intake duct length on the in-cylinder air motion in a motored diesel engine. SAE Paper No: 900057, 1990
18. P. Ramakrishna, K. Govinda and T. Venkata .Experimental Investigation on Diesel Engines by Swirl Induction with Different Manifolds. International Journal of Current Engineering and Technology SAE Paper 981020. E-ISSN 2277 – 4106
19. Torregrosa, A., Olmeda, P., Martín, J., & Degraeuwe, B. (2006). Experiments on the influence of inlet charge and coolant temperature on performance and emissions of a DI Diesel engine. *Experimental Thermal and Fluid Science*, 30(7), 633–641. doi: 10.1016/j.expthermflusci.2006.01.002
20. Cinar, C., Uyumaz, A., Solmaz, H., Sahin, F., Polat, S., & Yilmaz, E. (2015). Effects of intake air temperature on combustion, performance and emission characteristics of a HCCI engine fueled with the blends of 20% n-heptane and 80% isooctane fuels. *Fuel Processing Technology*, 130, 275–281. doi: 10.1016/j.fuproc.2014.10.026
21. Muthuvel, Mani & Govindan, Nagarajan & Sampath, S.. (2010). An experimental investigation on a DI diesel engine using waste plastic oil with exhaust gas recirculation. *Fuel*. 89. 1826-1832. 10.1016/j.fuel.2009.11.009.

APPENDIX A: CALIBRATION CERTIFICATES

OMEGADYNE INC.
An Affiliate of Omega Engineering, Inc.

PRESSURE TRANSDUCER
FINAL CALIBRATION

0.00 - 10.00 BAR
Excitation 28.000 Vdc

Job: Serial: 204832
 Model: PXM01MDO-010BARG5T Tested By: CHRIS
 Date: 9/20/2013 Temperature Range: +16 to +71 C
 Calibrated: 0.00 - 10.00 BAR Specfile: PXM01-5T

Pressure BAR	Unit Data Vdc
0.00	0.005
5.00	2.504
10.00	5.003
5.00	2.506
0.00	0.006

Balance 0.005 Vdc
 Sensitivity 4.998 Vdc
 80% Shunt 4.011 Vdc Change at 0.00 BAR (-INPUT to -OUTPUT)

ELECTRICAL LEAKAGE: PASS
 PRESSURE CONNECTION/FITTING: G 1/4 Female
 ELECTRICAL WIRING/CONNECTOR: Green = + Signal
 White = - Signal
 Black = - Excitation
 Red = + Excitation
 Blue & Orange = Shunt

This Calibration was performed using Instruments and Standards that are traceable to the United States National Institute of Standards Technology.

S/N	Description	Range	Reference	Cal Cert
0078/90-03	AUTO 1000 PSI DRUCK	0 - 10.00 BAR	C-2501	C-2501
US37034809	AT34970 DMM	Unit Under Test	C-3002	C-3002

Q.A. Representative : *Chris Ding* Date: 9/20/2013

This transducer is tested to & meets published specifications. After final calibration our products are stored in a controlled stock room & considered in bonded storage. Depending on environment & severity of use factory calibration is recommended every one to three years after initial service installation date.

Omegadyne Inc., 149 Stelzer Court, Sunbury, OH 43074 (740) 965-9340
 http://www.omegadyne.com email: info@omegadyne.com (800) USA-DYNE



CALIBRATION CERTIFICATE

CALIBRATION DATE 06/01/18

MODEL 700

TESTED BY [Signature]

SERIAL # 700422

THIS ANALYZER WAS SUCCESSFULLY ZEROED IN CLEAN AIR AND SUCCESSFULLY CALIBRATED USING 2% CERTIFIED ACCURACY NIST TRACEABLE SPAN GAS FOR THE MEASUREMENT OF THE FOLLOWING PARAMETERS AS NEEDED:

CALIBRATED SENSORS

CONCENTRATION

OXYGEN	<input checked="" type="checkbox"/>	0.00/20.9	%	NITROGEN/AIR
COMBUSTIBLES	<input type="checkbox"/>		%	CH ₄ balance NITROGEN
CARBON MONOXIDE	<input checked="" type="checkbox"/>	200/1930	PPM	CO balance NITROGEN
NITRIC OXIDE	<input checked="" type="checkbox"/>	200/990	PPM	NO balance NITROGEN
NITROGEN DIOXIDE	<input checked="" type="checkbox"/>	100	PPM	NO ₂ balance NITROGEN
SULFUR DIOXIDE	<input checked="" type="checkbox"/>	200	PPM	SO ₂ balance NITROGEN
DRAFT	<input checked="" type="checkbox"/>	5.00	"	W.C.
NDIR CARBON MONOXIDE	<input checked="" type="checkbox"/>	1.50	%	CO balance NITROGEN
NDIR CARBON DIOXIDE	<input checked="" type="checkbox"/>	10.3	%	CO ₂ balance NITROGEN
NDIR HYDROCARBONS	<input checked="" type="checkbox"/>	1000	PPM	C ₃ H ₈ balance NITROGEN

1320 LINCOLN AVE., HOLBROOK, NY 11741
 TEL: (516) 997-2100 (800) 695-3637
 FAX: (516) 997-2129

APPENDIX B: MATLAB CODINGS

```
% n is speed of the engine in rpm  
  
n=1800;  
  
% cytime is the cycle time. Cycle has 2 revolution  
  
% cycle time = (revolution in 1 cycle / engine speed (rps)) = 2/ (n/60)  
  
% cytime= 120/n  
  
cytime=120/n  
  
% mtime (s) is measuring time ( as you use on the oscilloscope)  
  
% in device it is (ms) it has be converted into (s)  
  
% horizontal axis unit is S  
  
mtime=.5  
  
% ncycle is number of cycle= measuring time / cycle time  
  
ncycl= (mtime)/(cytime)  
  
%angofcyc is the angleof all cycles represnted  
  
% one cycle is 720 degree so total angles for the all cycle is as below  
  
angofcyc=(ncycl*720)  
  
% the oscilloscope screen take 25000 point  
  
% to know the angle for each point divide the total angle by 25000  
  
thetastep=angofcyc/25000  
  
%tDCangle=tddtime  
  
% the clibration equation from volt to pressur as down  
  
p1750=(2.5188*v1750*100)*10^5;
```

```

figure(1)

plot(td1750,p1750)

% choosing filter by drawing frequency diagram

p_mags=abs(fft(p1750));

figure(2)

plot(p_mags)

xlabel('DFT Bins')

ylabel('Magnitude')

%plot first half of DFT (normalised frequency) as the freuency respons is

%mirror so we have to remove the reflection

num_bins = length(p_mags);

figure(3)

% numbins/2 to remove the mirror , for x axis (0: (numbins/2)-1) because

% fft function x axis start from one so we ttake out one

% to convert it into normlized one we divide the whole x axis like 1/(x

% axis) to make the domain from 0 to 1

plot([0:1/(num_bins/2 -1):1], (p_mags(1:num_bins/2)/(max(p_mags))))

% to convert the x-axis into Hz .freqHz = (0:1:length(X_mag)-1)*Fs(sampling/s)/N(length

of p-1750);

xlabel('Normalised frequency (\pi rads/sample)')

ylabel('Magnitude')

```

```

% butter build in function used as a low pass filter

[b a] = butter(3,0.03 , 'low')

%plot the frequency response (normalised frequency)

H = freqz(b,a, floor(num_bins/2));

hold on

plot([0:1/(num_bins/2 -1):1], abs(H), 'r');

% for visulizing the resuidals w will divide the magnitiude by 1.4*10^5

p_filtered1750 = filter(b,a,p1750);

plot(td1750,p_filtered1750)

pf1750=smooth( p_filtered1750,'moving',11);

t1750c=td1750+(-1*min(td1750));

% tdc1750=td1750+.25;

figure(4)

% h=plot(t1750c,pf1750,'b')

%%h=plot(t1750c,p_filtered1750,'b')

pfx=1:1:25000

plot(pfx,pf1750)

pfc=pf1750(1:5000)

plot(pfx(1:5000),pfc)

ind=find(pfc>450000,1)

h=plot(t1750c,pf1750,'r')

hold on

```

```

% plot(t1750c,v1750,'r')

% title({'1700 rpm'});

% grid on

th1750=0:thetastep:angofcyc;

thc1750=th1750(1:25000);

figure

h=plot(thc1750,pf1750,'b')

thcor=thc1750'

hold on

% % averaging the cycles

pavg=pf1750(ind:ind+600);

plot(thc1750(ind:ind+600),pavg)

% pfa=0;

% for n=1:4

% pfa=pf1750((3347*n):3347*(n+1))

% % pfa=pf1750((i*4167-4166):4166*i)

% end

% % pfavg=(pf1750(1:3348)+pfa)/5

plot(thc1750(ind:ind+600),pavg)

% % for i = 1:6

% subset = pf1750(i*4167-4166:4166*i)

% peak = max(subset);

```



```

% peaks(i) = peak;

% end

% averagepks=mean(peak)

dp=diff(pavg)

dtheta=thetastep

% dtheta=diff((thc1750)')

dp_dtheta=dp./dtheta

th2c1750=(thc1750(ind:ind+599)-0.204)'

plot(th2c1750,dp_dtheta)

% dp_dthetaf=smooth( dp_dtheta,'moving',11);

% plot(th2c1750,dp_dthetaf)

% % book solution

b=0.082 ; % engine bore (m)

S=0.086; % engine stroke (m)

% hsr=0.25; % half stroke (crank radius )to rod ratio, s/2

rc=18; % compression ratio

% We need to shift the the volume

Vtdc=pi/4*b^2*S/(rc-1); % volume at TDC

% % s is the distance between crank axis ans wrist bin axis

% % a is the offst or radius of crankshaft

% % r is connecting rod length

% % look pulkrabek internal combustion book page 36:42

```

```

r=131/1000;

a=S/2

s= a*cosd(thc1750)+sqrt((r^2)-((a)^2*(sind(thc1750).^2)));

s1=diff(s)

v=Vtdc+(pi/4*b^2)*(r+a-s);

plot(thc1750,v)

%dv/dtheta

vc1=v(ind:ind+600)

%dv=1.9118*10^-9

dv=diff(v);

dtheta=0.204

dv_dtheta=(dv./dtheta)'

% plot(th3c1750,dv_dtheta)

% heat release rate

y=1.3

pfavgcbar=pavg./(10^5)

plot(th2c1750,pfavgcbar(1:600))

%corrected TDC final

thetatdc=th2c1750-4

plot(thetatdc,pfavgcbar(1:600))

% dp_dthetatdc=dp_dtheta(3:3347)

% plot(thetatdc,dp_dthetatdc)

```

```

% vcor=vc1((3:3347)) % 3.9229*10^-5 is the volum that equal to 16.6 theta
% vcor1=vcor
%dv_dtheta1=dv_dtheta(3:3347)
%comp should be index of min volume in var vcc
pavgc=pavg(1:600)
comp=find(pavgc>4594599,1)
dv_dtheta1=dv_dtheta(1388+(281-comp):1987+(281-comp)) % both this and the equ
down must be the same dim this the problem you have to change as speed change from 170
to 1800
vcc=v(1388+(281-comp):1987+(281-comp))'
Q=((y/(y-1))*pavgc.*dv_dtheta1)+((1/(y-1))*vcc.*dp_dtheta)
plot(thetatdc,Q)
%plot(vcc,pavgc)
%comp2 should be index of min volume in var v
comp2=find(pfc>4594599,1)
vpv=v(12199+(2803-comp2):17198+(2803-comp2))
plot(vpv,pfc)
pmax=max(pavgc)

```